UNIVERSITY OF PAVIA

FACULTY OF ENGINEERING
DEPARTMENT OF CIVIL ENGINEERING AND ARCHITECTURE

MASTER'S DEGREE IN ENVIRONMENTAL ENGINEERING – RESILIENCE TO CLIMATE CHANGE EFFECT CURRICULUM (REACH)

MASTER THESIS

EXPERIMENTAL CALIBRATION AND VALIDATION OF SOIL MOISTURE SENSORS FOR AN ARDUINO-BASED SMART IRRIGATION SYSTEM IN VINEYARDS

Candidate:
Norbert NSHIMIYIMANA

Supervisor:
Prof. D. Ravazzolo

Academic Year 2025-2026

ABSTRACT

Climate change poses a significant challenge to global viticulture, as rising temperatures and increasing frequency of drought events intensify water scarcity and negatively affect grape yield and quality. In many wine-producing regions, particularly in Mediterranean climates, maintaining optimal soil moisture conditions has become increasingly difficult. In this context, the adoption of precision agriculture technologies and smart irrigation systems represents a key strategy for improving water-use efficiency and enhancing vineyard resilience.

This study investigates the experimental calibration and validation of WATERMARK 200SS soil moisture sensors integrated into an Arduino Edge Control platform for vineyard monitoring and irrigation management applications. To improve the robustness of the monitoring system, soil moisture data were complemented with meteorological observations and measurements from a low-cost capacitive soil moisture sensor. The research methodology followed a dual-phase approach, consisting of laboratory calibration under controlled moisture conditions and subsequent field validation in an experimental vineyard. During the laboratory phase, sensors were tested across different predefined moisture gradients using a homogeneous sand substrate, allowing the evaluation of sensor sensitivity, response consistency, and stability under controlled conditions. The calibration process also enabled the characterization of the relationship between electrical resistance and soil water tension. In the field validation phase, sensor performance was assessed under real environmental conditions, including natural rainfall events and controlled irrigation inputs, to evaluate their practical applicability in dynamic vineyard conditions.

The results demonstrate a strong agreement between laboratory and field measurements, confirming the reliability and robustness of the sensors across varying environmental conditions. The Watermark 200SS sensors were able to clearly distinguish between different soil moisture levels and showed high responsiveness to both irrigation and precipitation events through measurable variations in soil water tension. Compared to the low-cost capacitive sensor, the WATERMARK sensors exhibited more stable and consistent behavior, particularly under fluctuating moisture conditions.

Overall, the findings confirm that WATERMARK 200SS sensors represent reliable tools for real-time soil moisture monitoring in viticulture. Their integration within an Arduino-based system provides a cost-effective, scalable, and efficient solution for data-driven irrigation management. This approach contributes to optimizing water use, reducing unnecessary irrigation, and supporting sustainable vineyard management under current and future climate change scenarios.

ACKNOWLEDGEMENTS

First and foremost, I wish to express my profound gratitude to the Almighty God for His divine blessings, wisdom, and the strength that guided me through every stage of this academic journey.

I would like to extend my deepest and most sincere appreciation to my supervisor, Prof. D. Ravazzolo. I am profoundly grateful for his expert mentorship, his tireless support, and the scholarly vision he shared with me throughout this research. The completion of this thesis would not have been possible without his expertise and motivation. It has been a true honour to conduct this research under his distinguished guidance.

I also want to express my sincere gratitude to Prof. Roberto Valentino and Prof. Gabriella Petaccia. Their great support has been essential to my life and played a huge role in helping me achieve my dream of earning this master's degree. I am deeply thankful for their kindness and belief in me.

My thanks also go to the administration and faculty of the Department of Civil Engineering and Architecture at the University of Pavia. Thank you for providing a great work environment and the resources needed for my research. I also wish to thank all the lecturers who facilitated my academic growth during my master's degree studies.

I would like to extend my sincere thanks to Engineers Joseline Byukusenge, Fidele Twizerimana, Honore Ishimwe, and Gaspard Munyanganizi. Their exceptional technical expertise and constant availability were pillars of support throughout my postgraduate journey. I am deeply indebted to them for their guidance, which not only enriched my research but also profoundly shaped my academic path.

On a personal note, I give my heartfelt appreciation to my family, especially my mother, Aunts, and Uncle, for their endless love and encouragement. Their faith in my abilities has been the foundation of all my educational success.

Finally, I am grateful to my friends, colleagues, and classmates for their moral support and shared resilience. Our collective motto, "No Return, No Surrender," served as a constant reminder to persevere and move forward regardless of the challenges.

TABLE OF CONTENTS

LIST OF FIGURES

LIST OF TABLES

CHAPTER 1: INTRODUCTION

1.1 Climate change overview

The entire world faces the challenge of climate change and burning fossil fuels, cutting down forests and farming livestock are increasingly influencing the climate and the earth's temperature. This adds enormous amounts of greenhouse gases to those naturally occurring in the atmosphere, thereby increasing the greenhouse effect and global warming (website 1). Climate change affects all regions around the world. Polar ice sheets are melting, and the sea is rising. In some regions, extreme weather events and rainfall are becoming more common, while others are experiencing more extreme heat waves and droughts. Climate change is a very serious threat, and its consequences impact many different aspects of our lives. Due to the changing climate, many European regions are already facing more frequent, severe, and longer-lasting droughts. A drought is an unusual and temporary deficit in water availability caused by the combination of lack of precipitation and increased evaporation (due to high temperatures). Droughts often have knock-on effects, for example on transport infrastructure, agriculture, forestry, water, and biodiversity. They reduce water levels in rivers and groundwater, stunt tree and crop growth, increase pest attacks, and fuel wildfires. In Europe, most of the roughly EUR 9 billion annual losses caused by drought affect agriculture, the energy sector and the public water supply. Extreme droughts are becoming more common in Europe, and the damage they cause is also growing. With a global average temperature increase of 3°C, it is projected that droughts will occur twice as often, and absolute annual losses from droughts in Europe will increase to EUR 40 billion per year, with the most severe impacts in the Mediterranean and Atlantic regions. More frequent and severe droughts will increase the length and severity of the wildfire season, particularly in the Mediterranean region. Climate change is also expanding the area at risk from wildfires. Regions that are not currently prone to fires could become risk areas. Climate change is expected to lead an increase in precipitation in many areas. Increased rainfall over extended periods will mainly lead to fluvial (river) flooding, while short, intense cloudbursts can cause pluvial floods, where extreme rainfall causes flooding without any body of water overflowing. Climate change is also leading to indirect impacts on biodiversity through changes in the use of land and other resources. These may be more damaging than the direct impacts due to their scale, scope and speed. The indirect impacts include habitat fragmentation and loss; over-exploitation; pollution of air, water and soil; and the spread of invasive species. They will further reduce the resilience of ecosystems to climate change and their capacity to deliver essential services, such as climate regulation, food, clean air and water, and the control of floods or erosion. (Website 2).

Figure 1: *Composite representation of climate change impacts on the natural environment, illustrating (from left to right) urban flooding, forest wildfire intensification, and severe soil desertification (from website 2).*

The climate crisis has increased the average global temperature and is leading to more frequent high-temperature extremes, such as heatwaves. Higher temperatures can cause increased mortality, reduced productivity and damage to infrastructure. The most vulnerable members of the population, such as the elderly and infants, will be most severely affected. Temperature rises are also likely to influence phenology the behaviour and lifecycles of animal and plant species. This could in turn lead to increased numbers of pests and invasive species, and a higher incidence of certain human diseases (Website 2).

According to the European Commission (n.d.), the period 2015–2024 was the warmest decade recorded, with global average temperature reaching 1.55°C above pre-industrial levels in 2024. Human-induced global warming is presently increasing at a rate of 0.25°C per decade. An increase of 2°C compared to the temperature in pre-industrial temperatures is associated with serious negative impacts on the natural environment and human health and wellbeing, including a much higher risk that dangerous and possibly catastrophic changes in the global environment will occur. For this reason, the international community has recognised the need to keep warming well below 2°C and pursue efforts to limit it to 1.5°C.

1.2 The impact of climate change and stress on agriculture

Global climate change presents a significant challenge to the world today. Since 1850, the combined temperature of land and ocean has been increasing at 0.06 °C on average per decade, with the rate of warming more than three times faster than that since 1982, at approximately 0.20 °C per decade (NOAA National Centers for Environmental Information, 2024). Agriculture, as the foundation of human subsistence and development, is greatly impacted by rapid global climate change (Karki et al., 2020). Global warming not only leads to frequent extreme weather events, uneven precipitation, droughts, and floods, resulting in reduced crop yields, but also disrupts ecological balance and affects the prevention and control of crop pests and diseases (Monteleone et al., 2023). Moreover, climate change has caused soil degradation and scarcity of land resources, thereby impacting the sustainable development of agricultural production (Eekhout and de Vente, 2022). One of the most immediate and pressing challenges facing agricultural production is the direct impact of climate change on crop cycles, yield, and quality. These issues pose significant challenges to the stability, sustainability, and livelihoods of farmers. The ecosystem changes resulting from climate change, such as the increased frequency and intensity of extreme weather events, the decline in soil fertility, water scarcity, and changes in the occurrence patterns of pests and diseases, have profound implications for agricultural production. These indirect impacts may lead to a decrease in agricultural productivity and even trigger food security issues. As an integral component of global economic and social development, agriculture not only provides us with food and raw materials, but it also plays a dual role in global climate change. It serves as both a major source of greenhouse gas emissions and a potential domain for mitigating climate change (Al-Sadi et al., 2024).

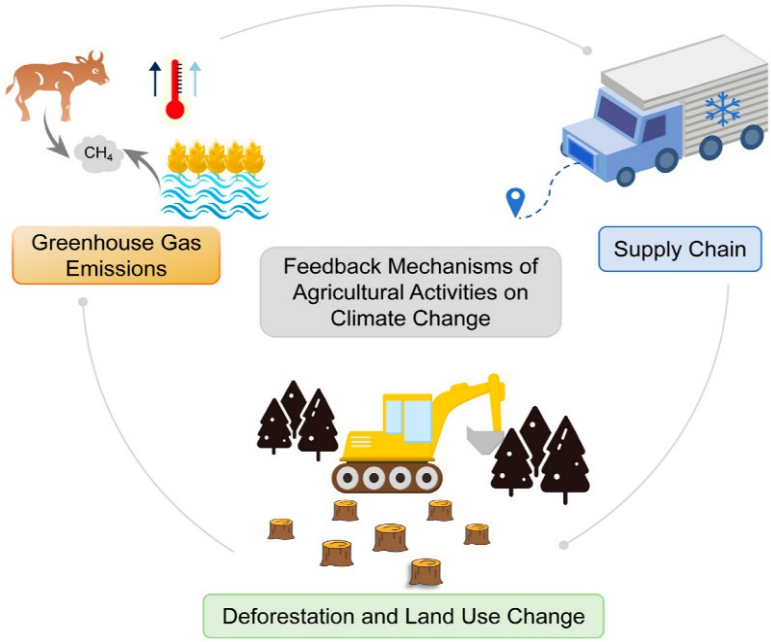

Figure 2: *Feedback mechanisms of agricultural activities on climate change. This cycle illustrates the interplay between greenhouse gas emissions (such as CH_4 from livestock), deforestation/land-use change, and supply chain logistics (including cold chain energy consumption). (Adapted from Al-Sadi et al. (2024)).*

Agricultural production is a significant contributor to greenhouse gas emissions, particularly of CO2, methane (CH4), and nitrous oxide (N2O), which exacerbate global warming. According to data from the Food and Agriculture Organization of the United Nations, livestock contributes to 14.5% of the total anthropogenic greenhouse gas emissions annually, playing a significant role in climate change. Secondly, manure management in livestock farming is also a significant source of CH4 and N2O. Furthermore, in modern agriculture, while the extensive use of fertilizers is a vital means of increasing crop yields, the production and application of fertilizers also result in greenhouse gas emissions. During fertilizer production, significant quantities of CO2 are generated due to the reliance on fossil fuels as energy sources, making this gas one of the primary drivers of global warming. In the process of fertilizer application, nitrogen fertilizers, a crucial component for ensuring food security, play a pivotal role. Deforestation and land use change are crucial aspects of agricultural activities affecting climate change. Large-scale deforestation is often carried out to expand agricultural land. Deforestation not only directly increases CO2 concentration in the atmosphere by reducing forest cover, but it also indirectly contributes to land degradation by altering land use, leading to soil degradation. The ability of soil to store organic carbon is a critical function, playing a vital role in climate regulation. Healthy soil structure can effectively sequester carbon, but when soil is degraded, stored organic carbon is released, further increasing greenhouse gas emissions. As the largest carbon

sink on land, soil stores more carbon than all biomass and the atmosphere combined. When land degrades, carbon and N2O stored in the soil are released into the atmosphere, making land degradation a major driver of climate change. The feedback mechanism of agricultural activities on climate change involves multiple aspects of the supply chain, with cold chain systems and food waste being two critical factors. On one hand, cold chain systems play a crucial role in the agricultural product supply chain. The high energy consumption of cold chain systems and the resource waste and greenhouse gas emissions resulting from food waste are significant drivers of climate change (Al-Sadi et al., 2024). Agriculture is the most vulnerable sector to climate change, owing to its large scale and sensitivity to weather parameters, thereby causing significant economic impacts (Mendelsohn, 2009). Changes in climatic variables such as temperature and rainfall significantly affect crop yields. The effects of rising temperatures, precipitation variation, and CO2 fertilization vary according to the crop, location, and magnitude of change in these parameters. An increase in temperature is found to reduce yields, while increased precipitation is likely to offset or reduce the impact of rising temperatures (Adams et al., 1998). As observed in Iran, crop productivity depends on adaptation capacity, crop type, climate scenario, and the CO2 fertilization effect (Karimi et al., 2018). The net revenue of farmers is found to decrease significantly with a decrease in precipitation or an increase in temperature in Cameroon. This factor, combined with poor policymaking, has led to low demand for Cameroon's agricultural exports, thereby causing fluctuations in national income (Molua and Lambi, 2007). Statistical evidence shows that temperature affects coffee yield in Veracruz, Mexico. It was also found that coffee production may not remain economically viable for producers in the coming years, with an estimated 34% reduction in current production (Gay et al., 2006). The effects of climate change on crop yields vary according to the area and irrigation application. Crop yields can be increased by expanding irrigated areas, which can have a detrimental effect on the environment (Kang et al., 2009). The rise in temperature is likely to reduce the yield of many crops by shortening their growth duration (Mahato, 2014). The aggregate production of wheat, rice, and maize is expected to decrease if both temperate and tropical regions experience a warming of 2°C (Challinor et al., 2014). Climate change generally has a greater impact on tropical regions, as tropical crops remain closer to their high-temperature optima and therefore experience higher levels of heat stress under elevated temperatures (Rosenzweig and Liverman, 1992). There has been a projection of more severe droughts in the near future due to climate change in most regions of the world, and an increase in drought-affected areas from 15.4% to 44.0% is projected by 2100. Africa is cited as the most vulnerable region. The yield of major crops in drought-prone areas is expected to be reduced by more than 50% by 2050 and by almost 90% by 2100 (Li et al., 2009). The loss of crop yields can increase food prices and have a significant impact on global agricultural welfare, with a 0.3% annual loss of

future global GDP by 2100 (Stevanović et al., 2016). However, Bosello and Zhang (2005) found that climate change has a limited influence on the global food supply, although developing countries will face severe negative consequences. In India, temperatures are predicted to rise between 2.33°C and 4.78°C, along with a doubling of CO2 concentration and longer heat waves, which could have a detrimental effect on the agricultural sector (Kumar and Gautam, 2014). Yield losses in three major cereal crops (rice, maize, and wheat) are projected to worsen by 10 to 25% with a 1°C increase in mean global surface temperature (Deutsch et al., 2018). In sub-Saharan Africa, the average crop yield is projected to decrease by 6–24% due to climate change (Waha et al., 2013). Plants' response to climate change varies according to species and developmental stage. There are species-specific thresholds, and plant responses, such as root elongation, changes in root growth angle, and yield reduction, vary among species (Gray and Brady, 2016). With increased CO2 content in the atmosphere, reduced transpiration has been observed in plants, leading to an increase in air temperature of 0.42 ± 0.02 K. This indirect physiological effect of elevated CO2, combined with a direct radiative effect, can increase land surface warming by 3.33 ± 0.03 K (Cao et al., 2010).

1.2.1 Effects of rising temperatures on vineyard agriculture

Vineyards are areas of land where grapes are grown. Grapes grow on vines that are supported by posts and wire, known as trellises. Grapes remain on the vines until they are ready to be picked or harvested. Grapes are grown based on their intended use. Some grapes are grown to be sold in food markets as table grapes, which are the grapes commonly found in grocery stores. Others are grown to be sent to wineries for wine production (Website 3).

According to data from the latest report on world viticulture issued by the Organisation Internationale de la Vigne et du Vin (OIV), the global area devoted to grapevine cultivation reached approximately 7.4 million ha in 2018, with a total wine production of 292 million hL. Five countries accounted for half of this area: Spain, China, France, Italy, and Türkiye. However, 50% of global wine production is concentrated in three countries: Italy, France, and Spain. From the same report, it can be observed that although the global vineyard area has undergone a slight decline in recent years, global grape production has shown a noticeable upward trend over the last two decades, with wine grapes accounting for 57% of total grape production. In fact, the monetary value of wine trade has increased continuously, reaching approximately 30,000 million euros in 2018, highlighting the high economic, environmental, and cultural importance of vineyards worldwide (Mirás-Avalos and Araujo, 2021).

Wine and wineries in Italy form a significant part of the country's culture. Italy is among the oldest wine-producing nations in the world and has one of the highest numbers of wineries. It is second only to France in wine production. It is also a country where meals are closely associated with the quality

of both food and wine. Italian wineries are among the world's largest exporters of wine. Italy has 20 wine regions, each with its own distinct characteristics and flavours. These regions are popular destinations for wine tourism (Website 4). It is second only to France in wine production. It is also a country where meals are closely associated with the quality of both food and wine. Italian wineries are among the world's largest exporters of wine. Italy has 20 wine regions, each with its own distinct characteristics and flavours. These regions are popular destinations for wine tourism (Website 4).

Figure 3: *The vineyards of Italy (Website 5).*

According to the OIV (International Organisation of Vine and Wine), Italy was the largest wine producer in the world in 2017 (Website 5). Warm climates suitable for grape production are characterized by an average seven-month growing season temperature between 17 and 19°C, while

hot climates range between 19 and 21°C. The seasonal growing degree day (GDD > 10°C) equivalent is approximately 1,500 to 2,000 for warm climates and 2,000 to 2,400 for hot climates. However, average temperatures alone do not fully describe climatic conditions. Warm climates are often characterized by the occurrence of hot days during the growing season. Hot days are defined as those in which the daily maximum temperature (Tmax) exceeds 35°C, a threshold above which many physiological processes begin to decline. Although the number of hot days is projected to increase under future climate scenarios, the western United States has already experienced as many days with Tmax > 35°C in 2021 and 2022 as those predicted for the end of this century. Higher temperatures also increase atmospheric evaporative demand, typically expressed as vapor pressure deficit, and accelerate transpiration from plant leaves. However, while rising temperatures increase plant water demand, irrigation water availability is decreasing. Dry soil conditions in spring, caused by reduced winter precipitation, may prevent vines from generating sufficient root pressure to restore the functionality of their vascular system, resulting in erratic budbreak, reduced shoot growth, and yield loss. Once canopy transpiration begins to drive water upward through the vine's xylem conduits, water deficit leads to a decline in leaf water potential (Ψl).

To protect themselves from drought stress, vines close their stomata at a higher Ψl than the threshold that triggers leaf wilting and abscission due to xylem cavitation. However, stomatal closure reduces photosynthesis, thereby limiting the amount of carbon available for export from the leaves. In vines grown on sandy soils, photosynthesis can decline within a few days after an irrigation event (Keller, 2023).

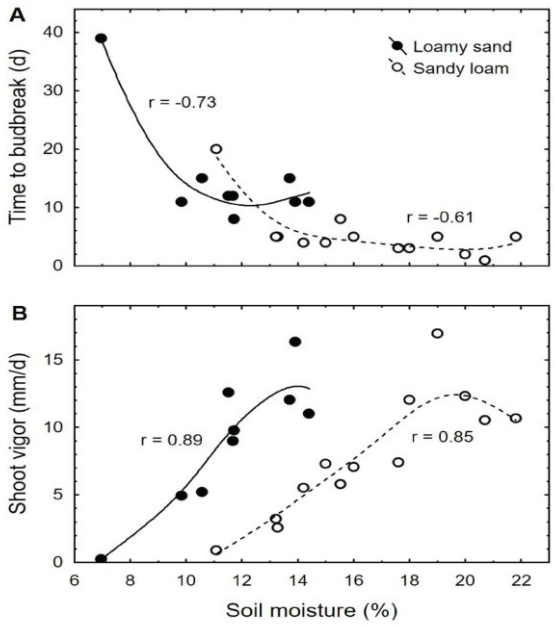

Figure 4: *Effect of soil type and soil moisture on (A) time to budbreak and (B) shoot Vigor (Source Keller, 2023).*

Effect of soil type and soil moisture on (A) time to budbreak and (B) shoot vigor of own-rooted Merlot grapevines grown in 27-L pots. Two different soils were collected at the Irrigated Agriculture Research and Extension Center in Prosser, Washington, based on the USDA soil classification (https://websoilsurvey.sc.egov.usda.gov), and then dried. Dormant two-year-old vines grown in pots were removed from cold storage, pruned to 10 buds, repotted in the two dry soils, transferred to a greenhouse (temperature range 12 to 30°C), and irrigated daily at approximately 1% (v/v), with target increments ranging from the permanent wilting point to field capacity for each soil type. Volumetric soil moisture was measured using time-domain reflectometry (HydroSense, Campbell Scientific). Time to budbreak was defined as the number of days from placement in the greenhouse to the appearance of green tissue on at least five buds. Shoot vigor was defined as the average growth rate over the first five weeks after budbreak (Keller, 2023).

Warmer temperatures extend the period during which the minimum temperatures required for vine physiological activity are reached, thereby increasing metabolic rates and affecting metabolite accumulation. However, this effect occurs only within certain limits, as net photosynthesis decreases at temperatures above 25°C, even under constant sunlight exposure. At such high temperatures, the replacement of starch by lipids in leaf chloroplasts has been reported in grapevines, and above 30°C, berry size and weight are reduced, while metabolic processes and sugar accumulation may cease completely. Although high temperatures accelerate grape maturation, their effect on final sugar accumulation is relatively limited. Temperatures around 30°C may lead to higher concentrations of suspended solids, but Brix levels above 24–25 are more likely due to concentration by evaporative water loss rather than increased photosynthesis or sugar transport from leaves and woody tissues. Combined with extended hang times aimed at optimizing aromatic maturity, climate change has introduced several important winemaking challenges related to grape composition. The main microbiological and technological challenges include higher temperatures of harvested grapes delivered to wineries, elevated environmental temperatures during fermentation, increased sugar and possibly potassium concentrations in grape berries, lower acidity levels, and higher pH values (De Orduna, 2010).

Climate change affects wine because its characteristics are strongly influenced by the climate and seasonal patterns of the region where grapes are grown. Seasonal temperature variations determine the phases of the plant life cycle. In addition, temperature plays a crucial role in fruit ripening, influencing the organoleptic characteristics and balance of wine. Water availability is also a key factor in high-quality wine production. Water availability is decreasing during the summer period, although this varies across regions. Conversely, in spring, extreme rainfall events are becoming more frequent, leading to soil erosion or flooding, sometimes accompanied by hail or late frost (Website 6).

1.2.2 The hydrological challenges in viticulture

Climate Dynamics and Physiological Response. Anthropogenic climate change, characterized by escalating mean temperatures and prolonged xerothermic periods, has significantly reduced water security across various Italian viticultural regions. Elevated thermal indices exacerbate environmental demand by accelerating soil water evaporation and enhancing plant transpiration rates. While Vitis vinifera is a Mediterranean species that exhibits relatively low water requirements and a high sensitivity to soil saturation (waterlogging), specific phenological stages require precise moisture levels to ensure vine longevity and yield quality. Historically, "moderate water stress", quantified by a soil water potential typically ranging between −30 and −60 kPa (or centibars), has been identified as a catalyst for premium red wine production. Empirical studies corroborate that controlled water deficits during fruit maturation (veraison) effectively reduce berry size. This increase in the skin-to-pulp ratio facilitates a higher concentration of polyphenols and enhances the aromatic complexity essential for aging potential. Conversely, for white cultivars, the threshold for water stress is significantly lower; excessive deficits often lead to premature leaf senescence and a loss of volatile precursors. Consequently, maintaining a narrow range of moderate stress is critical, as exceeding these physiological thresholds results in a rapid decline in metabolic efficiency and fruit quality.

Figure 5: *Vines under severe water stress (Source Website 6).*

Spatio-Temporal Variability and Adaptive Mechanisms. In practice, viticultural plots often exhibit significant intra-field heterogeneity; vines may display robust vegetative vigor in close proximity to

individuals exhibiting acute water stress symptoms. This variability is primarily governed by Soil Water-Holding Capacity (SWHC), which determines the volumetric water content available to the root system. SWHC can fluctuate substantially over short distances due to variations in soil texture, structure, and organic matter content. The phenomenon of physiological acclimation plays a decisive role in stress resilience. Vines established in high-resource environments develop hydraulic architectures, such as larger vessel diameters and higher stomatal conductance, optimized for high water consumption. When subjected to abrupt drought conditions, these "non-acclimated" vines lack the compensatory mechanisms (e.g., osmotic adjustment or restricted vegetative growth) found in vines grown under chronically resource-limited conditions.

Because of this high spatial variability in SWHC and the specific sensitivity of non-acclimated vines, a uniform irrigation approach is insufficient. Instead, an automated, sensor-driven system is required to provide site-specific water delivery, maintaining the precise soil water potential (kPa) necessary to optimize grape quality without risking plant mortality (Website 6).

1.3 Techniques for adapting to climate change affecting vineyard production

Grapevine phenology refers to the timing of its growth stages, which are highly sensitive to climatic conditions. The phenological characteristics of grapevines are crucial for viticultural planning and decision-making. Indeed, grape varieties must be well adapted to local climate conditions to ensure optimal growth and ripening. If harvest occurs too early, grapes tend to have high sugar content and low acidity, resulting in unbalanced wines. Conversely, when ripening occurs too late, grapes exhibit high acidity and low sugar content, often accompanied by unripe aromas. In the Northern Hemisphere, optimal ripening generally occurs during September, when days remain warm and sunny while nights are cooler. Adaptation to climate change represents a major challenge for the viticulture sector. From a temporal perspective, adaptation strategies and policies must address both short-term and long-term impacts. Furthermore, since each wine-growing region is characterized by unique environmental conditions, a thorough understanding of local factors and their interaction with regional climate is essential for identifying and prioritizing adaptation strategies at different temporal and spatial scales. Over the next century, winegrowers are likely to face increasing temperatures and changing rainfall patterns, which will significantly affect two main aspects of grape production. The first is grapevine phenology: as growth stages are expected to occur earlier, the shift of the ripening period toward warmer summer conditions will influence grape composition, including sugar and acidity levels, as well as aroma compounds. The second aspect is soil water availability: grapevines are expected to experience increased water stress due to rising temperatures, higher

evapotranspiration rates, and altered precipitation patterns. These changes are likely to have significant effects on grape quality and yield (Quénol et al., 2020).

Table 1: *Examples of possible types of adaptation responses to the continuation of climate change for a given plot (from Quénol et al., 2020).*

Adaptation measures	Effect on delaying grape ripening (days)	Adaptation measures	Water stress Intensity
Delaying pruning date	3-5	Cover crop species	Weak
Increasing trunk height	3-5	Soil tillage techniques	Weak
Reducing leaf area/ fruit weight ratio	5-12	Mulching techniques	Weak
Choice in rootstock variety	3-6	Trellising system	Medium
Clonal selection	3-8	Choice in rootstock variety	Medium
Choice in grapevine variety	10-25	Irrigation	Strong

These strategies range from short-term adjustments (e.g. in harvest management practices) to long-term adjustment, such as in varietal selection. In response to increasing temperatures and changing rainfall patterns, they vary therefore in nature and effectiveness, where long term measures in the choice in grapevine variety and the use of irrigation are the most effective (Figure 6). However, these long-term measures will likewise induce the greatest changes in wine style and quality.

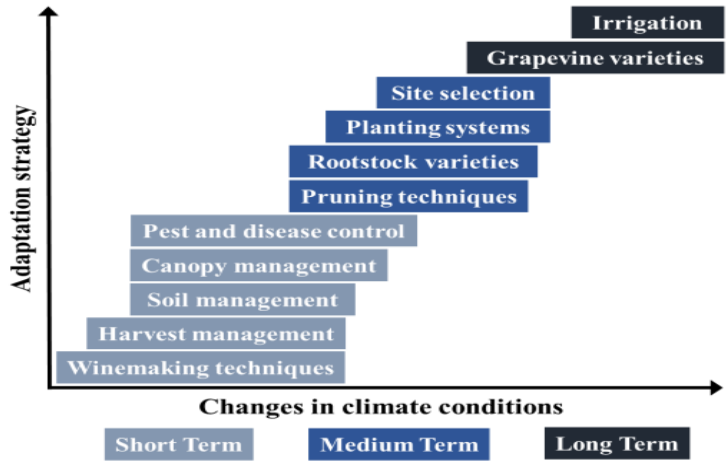

Figure 6: *Representation of different adaptation strategies to changes in climate conditions over the short, medium and long term (from Quénol et al., 2020).*

1.3.1 Short term adaptation options

A) Harvest management and winemaking practices

In the context of climate change, short-term adaptation strategies mainly involve annual management practices that allow rapid responses to seasonal variability in grape development and composition. First, harvest management plays a crucial role in adapting to changing climatic conditions. Adjustments in harvest timing, based on grape ripening dynamics, prevailing weather conditions, and risks such as grey rot, enable winegrowers to better manage interannual variability in grape quality and composition. Second, adaptation continues during the winemaking stage. Once grapes are harvested, specific oenological practices can be applied to compensate for variations in sugar content, acidity, and phenolic composition, thereby maintaining wine quality despite climatic fluctuations.

B) Soil management practices

Soil management practices are essential for regulating grapevine water availability, controlling vegetative growth, and reducing soil erosion. The most common strategies include soil tillage and cover cropping. In recent years, increasing environmental regulations in Europe have encouraged the adoption of alternative practices to chemical weed control. These alternatives include shallow tillage and the use of grass cover, selected according to soil type and climatic conditions. Shallow tillage helps reduce soil water evaporation during summer droughts, while grass cover improves soil structure, increases bearing capacity during periods of heavy rainfall, and helps limit excessive vine vigor. These management practices are expected to evolve further as the frequency and intensity of drought and heatwave events increase.

1.3.2 Short to medium term adaptation options

A) Management of frost risks

The strong relationship between local topography and frost occurrence means that frost protection strategies vary significantly across vineyard sites. Frost management can be divided into passive and active protection methods. Passive protection includes preventive measures implemented in advance, such as site selection, pruning strategies, and cultivar choice, aimed at reducing vineyard susceptibility to frost damage. Active protection involves direct interventions applied shortly before or during frost events, including wind machines, heaters, and over-vine sprinklers. Among these approaches, passive strategies are generally considered the most effective long-term solutions, particularly through careful site selection and the use of late-ripening grape varieties. Avoiding frost-prone low-lying areas and selecting suitable cultivars can significantly reduce frost-related risks (Quénol et al., 2020).

1.3.3 Medium term adaptation options

A) Choice of rootstocks and clones

Medium-term adaptation to climate change involves modifications to perennial vineyard components. One important strategy is clonal selection. Within the same grape variety, clones may exhibit differences in ripening time of approximately 8-10 days. This natural variability can be exploited during vineyard replanting to delay maturity and avoid harvesting during excessively hot periods. Another key strategy concerns rootstock selection. Rootstocks strongly influence vine behavior, including precocity, vigor, and water uptake capacity, and allow adaptation to different soil physical and hydrological properties. Rootstock choice complements site selection and represents a major tool for adapting vineyards to increasing water deficits. Resistance to drought varies considerably among rootstocks; for example, 140 Ruggeri and 110 Richter are known for their high drought tolerance. Current viticultural research focuses on developing new rootstocks with improved resistance to water stress. Importantly, adaptation through rootstock selection is environmentally sustainable and does not significantly increase production costs (Quénol et al., 2020).

B) Site selection

Local topographic and soil variability provides important opportunities for climate change adaptation. Microclimatic differences within small geographical areas can significantly influence vineyard performance and therefore must be systematically analyzed during viticultural planning. Topography, slope, and aspect can create substantial temperature differences within a vineyard, sometimes varying by several degrees between hilltops and valley bottoms. These variations allow growers to adapt cultivation practices according to local conditions. Similarly, soil texture and depth strongly influence water availability. Under increasing drought conditions, deeper soils with higher water-holding capacity are generally preferred. Soils with greater water reserves should be allocated to varieties sensitive to water stress, while more drought-resistant varieties may be planted in drier areas (Quénol et al., 2020).

1.3.4 Long term adaptation options

A) Choice of grape variety

In quality-oriented wine production, grape varieties must be well adapted to local climatic conditions, particularly regarding ripening timing. To prevent quality losses associated with excessive temperatures during ripening, strategies aimed at delaying phenological development are required. Plant material represents a key adaptation tool. Rootstocks that extend the growth cycle and late-ripening clones can delay maturity by approximately 7-10 days without significantly altering wine typicity. However, larger shifts in ripening time may require the introduction of late-ripening grape

varieties. While some traditional regions already possess suitable late-ripening cultivars, in other cases the introduction of non-local varieties may become necessary. This adaptation remains challenging in European appellation systems, where regulations often restrict the use of non-traditional varieties. Nevertheless, gradual experimentation with small proportions of alternative varieties may help producers prepare for future climatic conditions (Quénol et al., 2020).

B) Irrigation

Irrigation involves the controlled application of water to grapevines to maintain adequate soil moisture and prevent excessive water stress. Water availability directly affects photosynthesis, vegetative growth, and berry development. Under typical conditions, grapevines require approximately 250 mm of water during the growing season to avoid severe stress (Quénol et al., 2020). Several irrigation methods are used in viticulture, ranging from traditional surface irrigation to modern precision systems. Among these, drip irrigation provides the highest level of control, allowing precise water delivery to individual vines. Although installation costs are relatively high, drip irrigation significantly improves water-use efficiency. However, irrigation also presents environmental, economic, and social challenges. In regions where water resources are limited, irrigation of grapevines (traditionally considered drought-tolerant crops) must be carefully justified. Additionally, irrigation may promote soil salinization if winter rainfall is insufficient for salt leaching, which can negatively affect vine health. Therefore, when irrigation is necessary, deficit irrigation strategies are recommended to optimize water use while maintaining grape quality.

1.3.4 The methods used for irrigation in vineyards and the importance of irrigation in vineyards

Water availability is a fundamental factor in viticulture, as it directly influences both grape yield and fruit quality. The amount and timing of water supplied to grapevines play a critical role in regulating vine growth, berry development, and overall vineyard productivity. Although rainfall represents the least labor-intensive and most economical water source, increasing climate variability and altered precipitation patterns have made reliance on natural rainfall increasingly unreliable. During prolonged droughts and heatwaves, water deficits may occur, potentially limiting vine growth or, in severe cases, threatening plant survival depending on the phenological stage. In this context, irrigation represents an essential strategy for mitigating water stress in vineyards. Irrigation can be defined as the controlled application of water to crops to ensure adequate soil moisture and prevent excessive plant stress. In grape production, the main objective of irrigation is to supply water at the appropriate time and in suitable quantities to maintain optimal vine physiological conditions while avoiding over-irrigation. The selection of an irrigation method depends on several factors, including vineyard size,

topography, soil characteristics, and grapevine variety. The three main irrigation systems commonly used in vineyards are surface irrigation, sprinkler irrigation, and micro-irrigation.

Surface irrigation, also known as flood irrigation, is the oldest irrigation method historically used in agriculture. This technique involves distributing water across the vineyard surface, allowing infiltration into the soil primarily through gravity. Although this method requires minimal infrastructure and has relatively low installation costs, it provides limited control over water distribution uniformity. As a result, uneven water application may occur, leading to over-irrigation in some areas and significant water losses through evaporation and surface runoff.

Figure 7: *Irrigation sprinkler vineyard (from Website 7).*

Sprinkler irrigation distributes water through pressurized pipelines connected to sprinkler heads positioned throughout the vineyard. Water is sprayed into the air and falls onto the soil surface, simulating natural rainfall. Compared to surface irrigation, sprinkler systems offer improved water distribution and additional benefits, such as frost protection during critical periods in spring and autumn. However, this method remains less efficient in terms of precise water delivery to individual vines. Water losses due to evaporation are still significant, since water droplets travel through the air before reaching the soil.

Micro-irrigation, commonly referred to as drip irrigation, represents the most efficient irrigation method currently used in viticulture. In this system, water is delivered directly to the root zone of each vine through a network of pipes and emitters, applying small and controlled volumes of water. This targeted approach minimizes evaporation and runoff, significantly improving water-use efficiency. Despite its higher installation and maintenance costs, drip irrigation allows precise control

of irrigation scheduling and is therefore widely adopted in modern vineyards. Proper filtration systems are required to prevent emitter clogging and ensure long-term system performance.

Figure 8: *Drip-irrigation being applied to a Niagara vineyard in late summer.*

The key principle of successful vineyard irrigation management is to provide sufficient water to sustain vine. physiological functions while avoiding excessive vegetative growth. In regions characterized by low rainfall, irrigation is particularly important during early growth stages and dry summer periods. However, once fruit development begins, controlled water deficits are often desirable to promote smaller berries and improve the skin-to-pulp ratio, which enhances grape quality. If water stress becomes excessive, supplemental irrigation may still be necessary to prevent irreversible damage. Consequently, irrigation management aims to achieve a balance between water supply and controlled stress, integrating irrigation practices with other vineyard management strategies to optimize both water use and grape quality.

1.4 Determining management thresholds for irrigation

Irrigation management thresholds represent reference values used to define the upper and lower limits of allowable soil water depletion. These thresholds are essential for optimizing irrigation scheduling, as they help maintain soil moisture within a range that prevents both water stress and excessive water application. The appropriate depletion range depends on several factors, including soil type, crop characteristics, plant developmental stage, and management practices. In general, a common starting point is to manage soil water depletion between approximately 10% (wet threshold) and 40–50% (dry threshold) of available water.

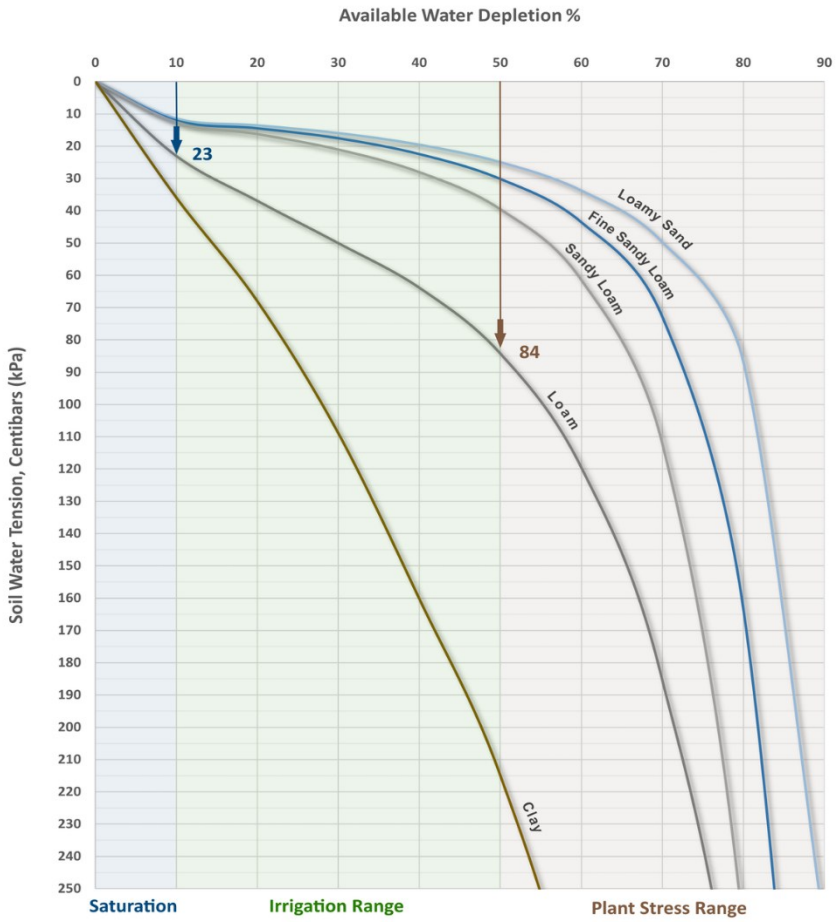

Figure 9: *Chart visually displays these relationships and provides a reference guide to assist in selecting appropriate threshold levels (from Website 8).*

Because soils differ in their water-holding capacity, the same level of water depletion corresponds to different soil water tension values depending on soil texture. For example, a 50% depletion in loam soil corresponds to approximately 84 centibars (CB) of soil water tension, whereas in sandy loam the equivalent value may be around 40 CB. Consequently, irrigation thresholds must always be interpreted in relation to soil-specific characteristics.

The relationship between allowable depletion and soil water tension can be visualized using reference charts, which support the selection of appropriate irrigation thresholds. The procedure for determining threshold values typically includes the following steps:

1) Identification of soil type: select the curve corresponding to the soil texture of the vineyard.

2) Determination of the wet threshold: starting from approximately 10% available water depletion, project vertically to the soil curve and then horizontally to the soil water tension axis. For example, in loam soil this value corresponds to approximately 23 CB.

3) Determination of the dry threshold: repeat the procedure using 40-50% depletion. In loam soil, this corresponds to approximately 84 CB.

Although the 50% depletion level is commonly used as a general reference, practical irrigation management often operates within a narrower range, typically between 30% and 50%, depending on irrigation strategy and crop requirements. Systems that apply smaller volumes of water more frequently generally adopt tighter depletion ranges to maintain more stable soil moisture conditions (adapted from Website 8).

1.5 Smart irrigation system using Internet of Things (IoT)

The term Internet of Things (IoT) refers to a network of uniquely identifiable embedded computing devices integrated into the global internet infrastructure. This framework enables seamless communication between physical hardware and digital systems through electronic sensors and wireless connectivity. By bridging the physical and digital environments, IoT technologies enable real-time data acquisition, processing, and synchronization across multiple platforms. Traditional farming practices often depend on irregular rainfall patterns and limited water availability, which can significantly affect agricultural productivity. Consequently, the adoption of automated irrigation systems has emerged as an effective solution. These systems use intelligent monitoring to evaluate soil moisture and fertility conditions, allowing water distribution to be adapted to the specific characteristics and requirements of the field.

The primary advantage of these technologies lies in reducing human intervention and minimizing risks associated with unpredictable rainfall patterns. Modern irrigation systems provide a reliable alternative to manual practices by incorporating automated decision-making processes for water management. Such systems typically operate through scheduled power cycles, optimizing energy consumption while maintaining adequate soil moisture conditions for crop growth. To implement this level of automation, the Arduino platform offers a robust and flexible solution. Arduino microcontrollers function as the central processing unit of the irrigation system, interfacing directly with soil moisture sensors and water pumps. Through dedicated algorithms, the microcontroller processes environmental data and activates irrigation hardware when necessary, providing a cost-effective and scalable approach for precision agriculture (Website 9). The use of IoT technologies is becoming increasingly widespread in the wine industry due to their advanced capabilities in data collection and analysis. In particular, IoT sensors are widely applied in vineyard monitoring and wine production, providing growers with valuable information to optimize grape quality and reduce resource waste. These sensors collect data related to climatic variables such as temperature, humidity, solar radiation, and wind conditions. The collected information supports decision-making processes by enabling the prediction of production trends, monitoring plant health, and facilitating timely interventions against diseases or infestations. Additionally, IoT-based soil moisture monitoring helps

farmers optimize irrigation scheduling, thereby reducing unnecessary water consumption and improving overall vineyard management efficiency (Website 10).

Water scarcity remains one of the major challenges affecting irrigation systems worldwide. For this reason, the implementation of smart irrigation systems capable of applying water precisely according to crop requirements has become increasingly necessary. Water management is a critical component of irrigation, and modern systems aim to reduce water consumption compared with traditional approaches. Smart irrigation not only reduces water use but also ensures that water is supplied according to real-time plant needs, thereby improving agricultural efficiency and reducing operational risks. These systems continuously monitor weather conditions, soil moisture levels, and reservoir water status through wireless sensors. Traditional irrigation methods, such as flood, manual, and surface irrigation, are characterized by low efficiency, with water losses ranging from 20% to 70% due to evaporation, deep percolation, and the lack of real-time monitoring. In contrast, smart irrigation techniques (particularly those utilizing IoT-based soil moisture sensors, climate-integrated automated controllers, and precision drip systems) can reduce water losses by up to 95%. This is achieved by delivering the precise volume of water required by the plant only when sensors detect that moisture levels fall below a defined threshold. By replacing fixed schedules or human-dependent irrigation practices with a sensor-based framework (using technologies such as Arduino or NodeMCU microcontrollers), these systems ensure optimal resource use and significantly higher application efficiency compared to conventional agricultural practices (Website 11).

1.6 Research Objectives

Climate change represents a major challenge for viticulture worldwide. Increasing temperatures and changes in precipitation patterns are expected to intensify water deficits in many wine-producing regions, with direct consequences for vine physiology, yield, and grape quality (van Leeuwen and Darriet, 2016). As discussed in the previous sections, maintaining grape quality under warmer and drier conditions requires careful control of vine water status. In practice, irrigation is increasingly considered a key adaptation measure; however, its effectiveness depends on applying the right amount of water at the right time, while avoiding both excessive irrigation and severe water stress.

Precision irrigation supported by real-time monitoring technologies provides a promising approach to improving water-use efficiency and supporting decision-making under highly variable field conditions. In particular, soil moisture monitoring is essential for translating irrigation thresholds into actionable management decisions, especially in vineyards where soil heterogeneity and plant responses can vary significantly over short distances. However, smart irrigation systems are only as reliable as the sensors that provide input data. If soil moisture measurements are inaccurate or

unstable, irrigation decisions may be misleading, potentially resulting in yield losses, reduced grape quality, or unnecessary water consumption. Therefore, sensor calibration and validation are critical prerequisites for implementing automated irrigation strategies based on soil moisture measurements. The smart irrigation monitoring platform considered in this study is based on an Arduino Edge Control system designed to integrate multiple environmental sensors for vineyard applications. Within this multi-sensor architecture, the present research specifically focuses on soil moisture sensors, which represent a crucial component for assessing soil water availability and supporting irrigation scheduling.

This study is centred on the experimental calibration and validation of these soil moisture sensors, following a structured workflow that reflects the practical development of the monitoring system.

First, the soil moisture sensors were connected to the Arduino Edge Control board, and the monitoring system was configured. During this phase, the Arduino script was developed and refined to ensure reliable sensor acquisition and improved wireless stability for continuous monitoring.

Subsequently, the data acquisition protocol was defined by setting the measurement interval to one reading every 15 minutes, balancing temporal resolution with system reliability. After completing system configuration, an indoor laboratory calibration was performed under controlled conditions using four plastic containers filled with sand and prepared with different water contents to reproduce distinct moisture levels.

Finally, the calibrated sensors were evaluated under real environmental conditions through an outdoor test in an experimental vineyard, where sensors were installed in four potted grapevines to monitor soil moisture dynamics within the substrate. Through this combined indoor-outdoor approach, the study assesses sensor responsiveness, stability, and applicability within a smart irrigation monitoring framework.

The specific objectives of this study are:

- **System integration:** to connect soil moisture sensors to the Arduino Edge Control platform and configure a stable monitoring setup within a multi-sensor smart irrigation architecture.
- **Code development and data transmission stability:** to develop and refine the Arduino script to ensure reliable sensor acquisition and stable data transmission during continuous operation.
- **Data acquisition protocol:** to define and implement an appropriate measurement interval (15-minute logging) through code optimization to support consistent monitoring of soil moisture dynamics.
- **Indoor calibration:** to calibrate soil moisture sensors under controlled indoor

conditions using sand substrates with known water contents, in order to characterize sensor response across distinct moisture levels.

- **Outdoor validation:** to evaluate the performance of the calibrated sensor under real environmental conditions in an experimental vineyard using one potted grapevine, assessing sensor stability and practical applicability.
- **Assessment for smart irrigation applications:** to assess the suitability of the calibrated soil moisture sensors as reliable components for data-driven irrigation monitoring and future automation of irrigation decisions in vineyard management.

Chapter 2. MATERIALS AND METHODS

2.1 Arduino-based monitoring system

The monitoring platform used in this study was developed using the Arduino Edge Control system, which is specifically designed for precision agriculture and remote environmental monitoring applications. The Arduino Edge Control board served as the central unit responsible for sensor integration, data acquisition, and overall system operation. This platform provides modular connectivity for multiple sensors and actuators, making it suitable for smart irrigation and environmental monitoring in agricultural environments. One of the main advantages of the Arduino Edge Control system is its ability to integrate different types of sensors while maintaining low power consumption and reliable operation under remote field conditions. The board allows the connection of several environmental sensors used to monitor key variables relevant to irrigation management, such as soil moisture, temperature, and other environmental parameters. In this study, the system was specifically configured to monitor soil moisture conditions.

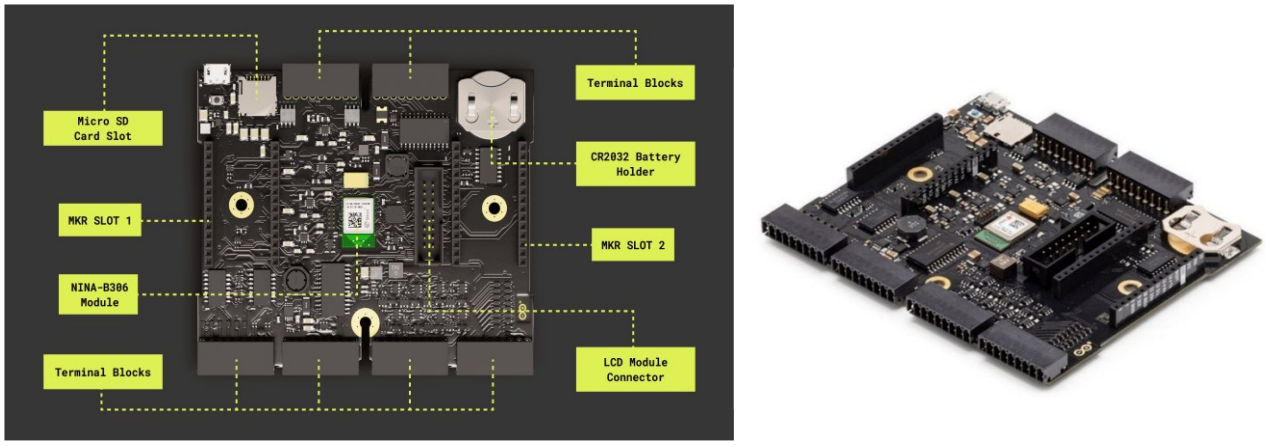

Figure 10: *Arduino Edge Control (from Website 13).*

A data acquisition protocol was implemented within the Arduino script to regulate the measurement frequency of the sensors. After several adjustments to the code, the monitoring interval was set to one measurement every 15 minutes.

The monitoring system was powered using a sealed lead-acid battery (12 V, 7 Ah). The Arduino Edge Control board can operate with an external voltage supply ranging from 6 to 20 volts; however, stable operation is recommended within a range of 7 to 12 volts to avoid voltage instability and overheating of the internal voltage regulator (Website 14).

A USB cable was used during the setup phase to connect the Arduino board to a laptop for uploading the program, testing system functionality, and debugging the code before field deployment.

Figure 11: *YUASA lead acid battery NP7-12 (from Website 14).*

2.2 Soil moisture sensors

Soil moisture monitoring in this study was carried out using WATERMARK 200SS soil moisture sensors, which are widely used in agricultural monitoring systems to measure soil water tension. These sensors belong to the category of granular matrix sensors, which estimate soil moisture conditions based on changes in electrical resistance within a porous matrix. Each sensor contains a granular material with a controlled composition that absorbs water from the surrounding soil. As soil moisture increases or decreases, the electrical resistance of the matrix changes accordingly. The sensor converts these resistance variations into measurements of soil water tension, expressed in centibars (CB). Compared with traditional gypsum block sensors, the WATERMARK 200SS sensor offers improved durability and reduced sensitivity to variations in soil salinity. As a result, it is capable of providing stable readings over extended periods and can remain permanently installed in the soil with minimal maintenance requirements. The sensor also operates with low power consumption, making it well suited for integration into IoT-based monitoring systems (Website 7).

Figure 12: *Example of the WATERMARK 200SS sensors (from Website 7).*

To interpret soil water tension measurements, general reference ranges are commonly used. Soil conditions can be broadly classified according to the following ranges:

- 0-10 centibars: saturated soil conditions
- 10-30 centibars: adequately moist soil
- 30-60 centibars: optimal irrigation range for many crops
- 60-100 centibars: increasing soil dryness
- 100-200 centibars: severe soil water deficit conditions

Although these ranges provide general guidelines soil moisture interpretation often requires site-specific calibration because soil texture, structure, and root distribution may influence sensor response (Irrometer Company, n.d.).

Several soil water concepts are also useful for understanding the meaning of these measurements. Field capacity refers to the soil moisture level remaining after gravitational drainage has occurred, when the soil retains water against gravity but is not saturated. The permanent wilting point represents the moisture level at which plants can no longer extract sufficient water to maintain physiological activity, typically corresponding to approximately 1,500 centibars. The difference between these two values represents the available water, which corresponds to the amount of soil water that can be used by plants (Website 8).

2.3 Software used for data collection and analysis

The integration of the Arduino Edge Control with the four WATERMARK 200SS soil moisture sensors required a robust software environment for code development, debugging, and real-time data acquisition. For this study, the Arduino Integrated Development Environment (IDE) 2.3.6 was used. This version represents a significant evolution from legacy editors, offering a modernized interface designed to enhance the efficiency of complex engineering projects.

As illustrated in Figure 13, the IDE features a dedicated sidebar that centralizes the most critical development tools:

- Core operations: the “Verify” and “Upload” functions allow for the compilation of the C++ based sketches and their subsequent deployment to the Edge Control hardware.
- Hardware and library management: the “Boards Manager” was essential for installing the specific packages required for the Arduino Edge Control ecosystem. Simultaneously, the “Library Manager” provided access to specialized sensor libraries, facilitating the conversion of raw resistance values from the Watermark sensors into soil tension (kPa) measurements.
- Data visualization and debugging: a pivotal feature for this thesis was the integrated “Serial Monitor” and “Serial Plotter”. These tools enabled the simultaneous monitoring of four

distinct sensor variables in a single console. The Serial Plotter, in particular, allowed for the visual identification of voltage peaks and moisture trends during the experimental characterization phase without the need for external data-logging software.

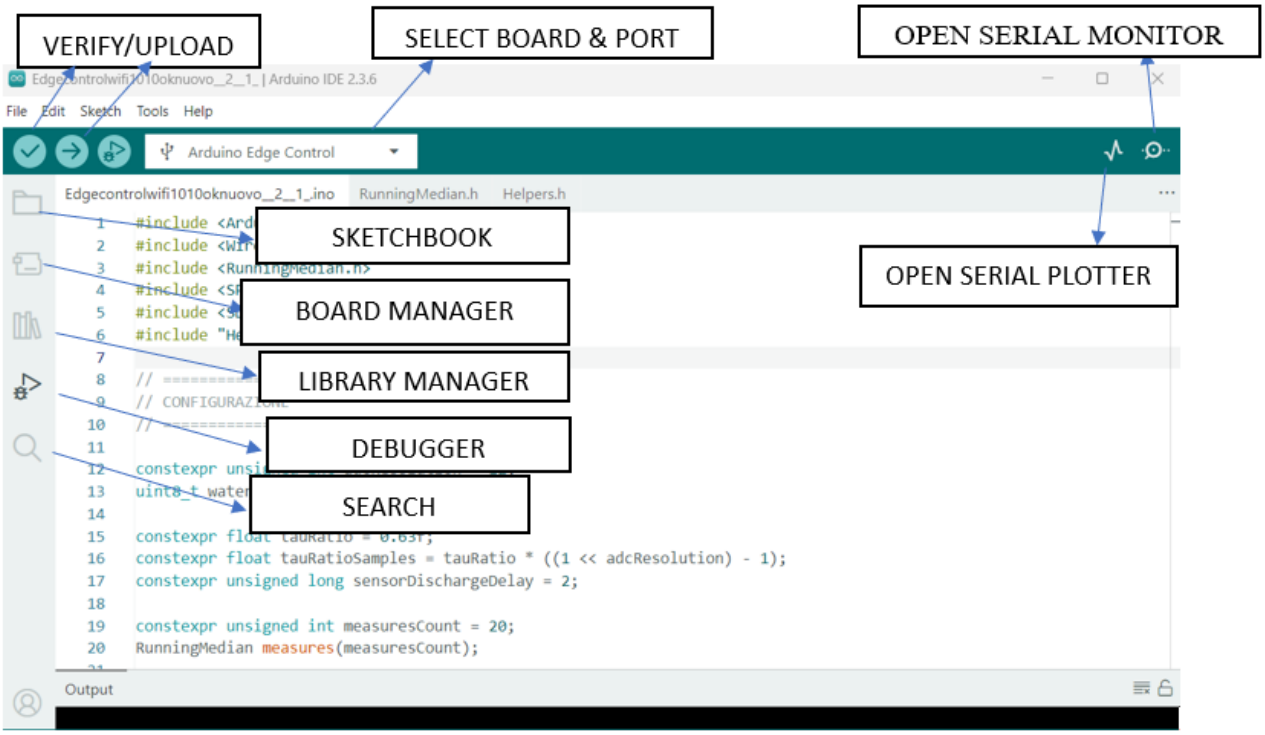

Figure 13: *Interface overview of the Arduino Integrated Development Environment (IDE) Version 2.3.6.*

The IDE 2.3.6 operates with a unified workspace, meaning the Serial Monitor is integrated directly into the editor. This layout allowed for real-time code adjustments based on the live feedback received from the soil-water matrix, ensuring high precision in the automated irrigation logic (Website 17).

2.4 Design, assembly, and testing of the smart irrigation system

The Arduino Edge Control, and four WATERMARK 200SS soil moisture sensors, and the YUASA NP7-12 lead-acid battery were interconnected according to the designated circuit layout. All components were wired to their respective terminals, following the J (jumper) reference points on the board to ensure correct polarity and electrical continuity. The electrical connections followed standard colour coding: the red wire carried the positive voltage, while the black wire represented the ground (GND) connection. The GND served as the electrical reference point (0 V), relative to which all voltage levels were measured. This configuration established the potential difference required to enable sensor operation, data acquisition, and overall system functionality. The YUASA NP7-12 lead-

acid battery served as the main power source, providing a stable 12 V DC supply. The positive terminal was connected to the BATT+ pin, while the negative terminal was connected to the GND pin of the J11 connector on the Arduino Edge Control board, as shown in Figure 14. The board then distributed the supplied voltage to the connected components, ensuring stable and consistent operation.

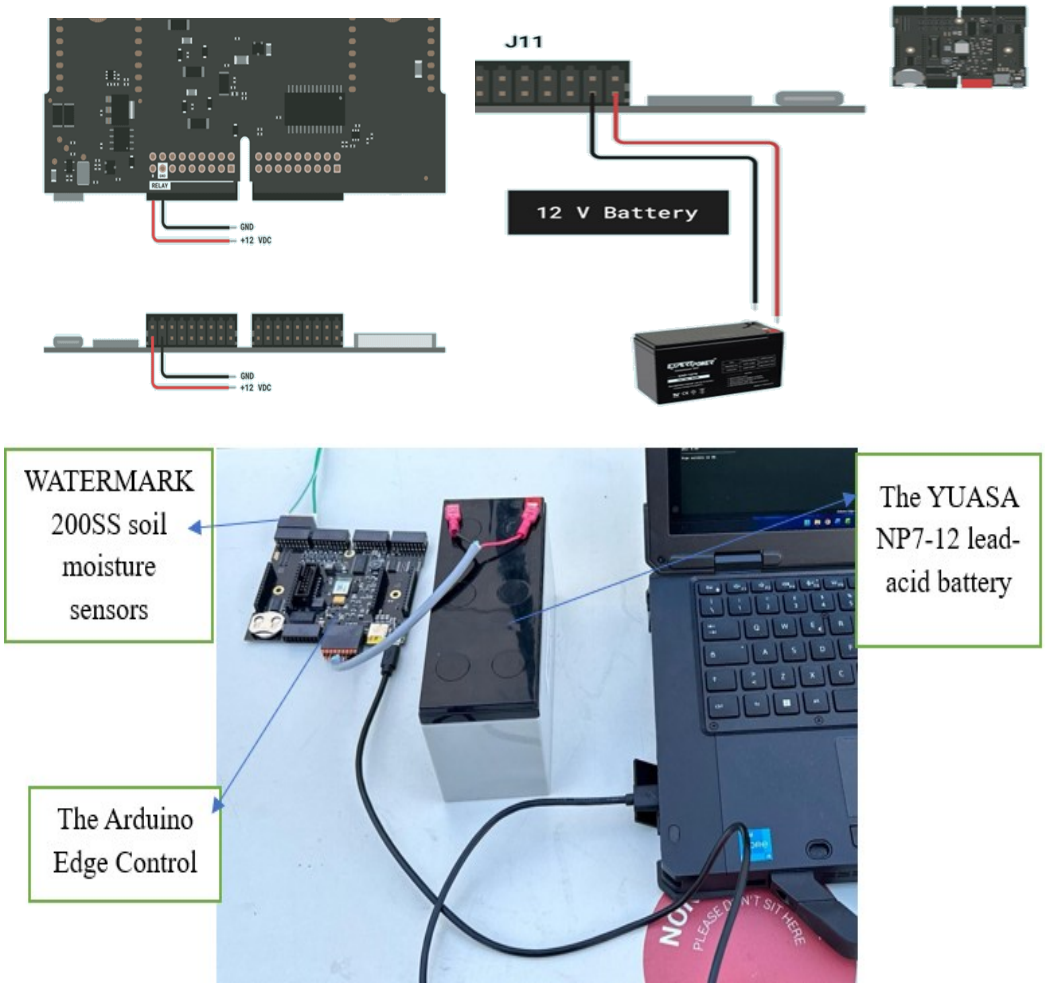

Figure 14: *Hardware configuration of the experimental setup, illustrating the integration of the Arduino Edge Control with Watermark 200SS sensors, and the 12V lead-acid battery power supply.*

The four Watermark 200SS sensors were connected to a terminal block, which acted as the interface between the sensors and the Arduino Edge Control board. One terminal of each sensor was connected to the common ground line, while the other terminals were connected individually to sensor input channels 1–4 on the J8 connector (Figure 15). This configuration enabled simultaneous monitoring of soil water tension at four measurement points, allowing spatial comparison of sensor responses across the experimental setup.

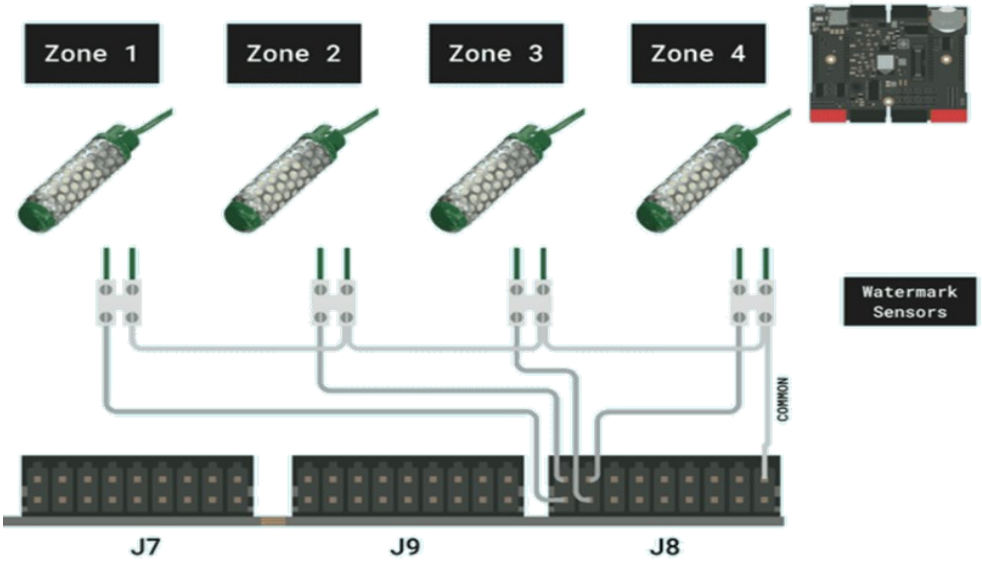

Figure 15: *Connection diagram of the four Watermark 200SS soil moisture sensors to the Arduino Edge Control board. (from Website 16).*

2.5 Development of the automated irrigation control and monitoring system

The precision water management system was developed within the Arduino IDE 2.3.6 environment, using the Arduino Edge Control as the primary microcontroller for local data acquisition and processing. To quantify soil moisture dynamics, the WATERMARK 200SS sensors were integrated into the system and referenced to experimental baseline conditions; the system computes sensor outputs by capturing the time response associated with reaching defined electrical thresholds during the measurement routine. For immediate on-site diagnostics, an integrated LCD interface was used to display soil-related variables and system status messages in real time.

2.6 System configuration and library integration

The firmware for the vineyard monitoring system was designed to support accurate data acquisition and protect the hardware during repeated measurements. To capture fine changes in sensor response, the Arduino Edge Control analog acquisition was configured at 12-bit resolution, increasing measurement granularity for the WATERMARK 200SS sensors. Because agricultural monitoring environments can be affected by electrical interference and sporadic signal spikes, the *RunningMedian.h* library was used to stabilize the readings. Instead of relying on a simple arithmetic mean (which can be skewed by outliers), the library evaluates a window of 20 measurements and selects the median value, effectively filtering random noise and improving the stability of the final output. To reduce polarization effects during sensor reading, the *Arduino_EdgeControl.h* library implements a “pseudo-AC” technique by alternating the excitation direction during measurements.

The raw timing/resistance-related outputs were then converted into standardized soil tension units (centibars) using formula routines stored in *Helpers.h*. Sensor outputs were organized through a structured format defined in *SensorValues.hpp* and transmitted every 30 minutes; this was later adjusted to 15-minute intervals to improve data accuracy.

```
16  #include <Arduino_EdgeControl.h>
17  #include <Wire.h>
18  #include <RunningMedian.h>
19
20  #include "SensorValues.hpp"
21  #include "Helpers.h"
```

The following part of the Arduino sketch corresponds to the initial configuration of the WATERMARK 200SS sensors. In this phase, the resistance thresholds were defined between 200 Ω and 35,000 Ω to establish functional operating boundaries for soil water tension measurements. In addition, the code defined a 30-minute interval (1,800,000 ms) for the communication routine.

```
30  // Thresholds for Watermark sensors
31  const long open_resistance = 35000, short_resistance = 200, short_CB = 40, open_CB = 255, TempC = 28;
32  // Watermark sensor channels
33  uint8_t watermarkChannel[4] = { 0, 1, 2, 3 };
```

```
45  // Interval for sending data via I2C (30 minutes)
46  unsigned long previousMillis = 0;
47  const long interval = 1800000; //30 minutes in ms
```

```
157   * Main Loop: Sensor management, water flow, LCD updates, and valve control.
158   */
159  void loop() {
160    delay(1800000);
161    detectTaps();
162    tapsHandler();
163    // Reset daily accumulators at midnight
164    if (getLocalhour() == " 00:00:00") {
165      Serial.println("Resetting accumulators every day");
166      vals.z1_on_time_local = 0;
167      // vals.z2_on_time_local = 0;
168      //vals.z3_on_time_local = 0;
169      //vals.z4_on_time_local = 0;
170      delay(1000);
171     }
```

The management and calibration of humidity sensors are primarily conducted through the functions *WatermarkCal, WatermarkGet, CalcCB, and readWatermark*.

A) The *WatermarkCal* function identifies the channels associated with the WATERMARK sensors and initializes the calibration routine. As implemented, the system measures sensor response time by recording the interval between a high-signal trigger and the moment the analog reading reaches the *tauRatioSamples* threshold at 12-bit resolution. To improve robustness, these measurements are filtered through the *RunningMedian* library via the calibs object. This step reduces the influence of transient electrical noise and outliers, producing stable reference values used by subsequent functions to compute soil moisture-related indicators.

```
291   * Calibrates a Watermark channel by recording response times
292   */
293  void WatermarkCal(uint8_t WK_ch) {
294    Watermark.disable();
295    Watermark.commonMode(INPUT);
296    Watermark.calibrationMode(OUTPUT);
297   for (unsigned int i = 0; i < measuresCount; i++) {
298      Watermark.calibrationWrite(HIGH);
299      unsigned long start = micros();
300      while (Watermark.analogRead(WK_ch) < tauRatioSamples)
301        ;
302      unsigned long stop = micros();
303      Watermark.calibrationWrite(LOW);
304     Watermark.fastDischarge(sensorDischargeDelay);
305     calibs.add(stop - start);
306    }
307  }
```

B) The *WatermarkGet* function supports real-time acquisition by enabling the sensor and recording channel-specific response times in microseconds. It iteratively triggers the excitation signal, measures the elapsed time until the threshold is reached, and stores the outputs in a measures object for filtering and further processing.

```
 * Measures a Watermark channel and records times (in microseconds) for detection
 */
void WatermarkGet(uint8_t WK_ch) {
  Watermark.enable();
  Watermark.commonMode(OUTPUT);
  Watermark.calibrationMode(INPUT);
  for (unsigned int i = 0; i < measuresCount; i++) {
    Watermark.commonWrite(HIGH);
    unsigned long start = micros();
    while (Watermark.analogRead(WK_ch) < tauRatioSamples)
      ;
    unsigned long stop = micros();
    Watermark.commonWrite(LOW);
    Watermark.fastDischarge(sensorDischargeDelay);
    measures.add(stop - start);
  }
```

C) The *CalcCB* function converts the processed sensor values into soil water tension expressed in centibars (CB). It applies equations conditioned on resistance ranges and temperature terms to preserve consistency across the operating domain. The function also detects fault conditions (e.g., short circuits or open circuits) by comparing readings with predefined resistance limits.

```
 * Converts Watermark sensor reading to centibars (CB)
 */
int CalcCB(int res) {
  int CB = 0;
  if (res > 550) {
    if (res > 8000) {
      CB = -2.246 - 5.239 * (res / 1000.0) * (1 + 0.018 * (TempC - 24.0))
      - 0.06756 * (res / 1000.0) * (res / 1000.0) * ((1 + 0.018 * (TempC - 24.0)) * (1 + 0.018 * (TempC - 24.0)));
    } else if (res > 1000) {
      CB = (-3.213 * (res / 1000.0) - 4.093) / (1 - 0.009733 * (res / 1000.0) - 0.01205 * (TempC));
    } else {
      CB = ((res / 1000.0) * 23.156 - 12.736) * (1 + 0.018 * (TempC - 24.0));
    }
  } else {
    if (res > 300) {
    CB = 0;
    }
    if (res < 300 && res >= short_resistance) {
      CB = short_CB;
      // Error code for short circuit
    }
  }
  if (res >= open_resistance) {
    CB = open_CB;
    // Error code for open circuit
  }
  return abs(CB);
}
```

D) The *readWatermark* function coordinates calibration and acquisition steps for the WATERMARK 200SS sensors. It updates system variables using the calculated values and manages real-time monitoring by outputting processed results to the display, providing a direct transition from raw signal acquisition to user-readable soil moisture indicators.

2.7 Relationship between electrical resistance, soil water tension, and soil moisture status for WATERMARK 200SS sensors

To evaluate the performance of the calibrated sensors under real environmental conditions in an experimental vineyard using one potted grapevine, assessing sensor stability and practical applicability. The standard range for a granular matrix sensor (specifically the WATERMARK 200SS) defines the relationship between the electrical resistance in Ohms and the soil water tension in centibars (CB). The sensor's electrical resistance and the corresponding soil water tension is presented in Table 2 and the relationship is inversely proportional (as resistance increases, moisture decreases) and non-linear. Even one 1 CB is equal to 1 Kpa.

Table 2: *Standard range of electrical resistance and corresponding soil water tension values across varying soil moisture gradients*

Soil Status	Resistance (Ω)	Tension (CB / kPa)	Interpretation
Saturated	0 – 550	0 – 9	Soil is too wet; no air for roots.
Field Capacity	550 – 2,800	10 – 30	Ideal "bucket" of water; easily available.
Adequate	2,800 – 9,000	31 – 60	Good moisture: irrigation usually starts here.
Drying out	9,000 – 15,000	61 – 100	Stress begins for sensitive plants (e.g., vegetables).
Dry	15,000 – 35,000	101 – 200	Very dry; critical for drought-tolerant crops.
Max Limit	> 35,000	> 200	Sensor begins to lose contact with soil.

2.8 Indoor calibration of soil moisture sensors

Before installing the sensors in the vineyard, a calibration experiment was conducted under controlled laboratory conditions in order to evaluate the response of the soil moisture sensors to different moisture levels.

The calibration setup consisted of four plastic containers filled with sand, each prepared with a different amount of water. The objective of this setup was to reproduce a range of soil moisture conditions under controlled conditions. Sand was selected as the calibration medium because of its relatively homogeneous texture and its ability to produce clearly distinguishable moisture gradients.

Each container was filled with sand and water was added in controlled quantities to create four different moisture conditions. The soil moisture sensors were then inserted into the containers and connected to the Arduino monitoring system. Sensor readings were recorded through the monitoring platform, allowing the response of each sensor to be observed under different moisture levels.

This indoor calibration experiment allowed the evaluation of sensor sensitivity, measurement stability, and consistency between sensors. Observing sensor behavior under controlled moisture conditions also served as a functional check prior to deployment in the experimental vineyard.

2.9 Preparation of materials for testing the watermark sensors

The preparation and installation of the WATERMARK soil moisture sensors were conducted in accordance with the manufacturer's specifications (Irrometer Co. Inc., 2021) to support accurate readings and reliable performance during measurements. The preparation process involved gathering all materials and equipment necessary for calibration and testing. Each sensor was carefully inspected to confirm that it was clean, undamaged, and functioning properly prior to testing.

2.9.1 Preconditioning and hydration protocol

To support accurate measurements, a standardized conditioning protocol was implemented prior to installation. This procedure was based on capillary hydration of the internal granular matrix while preventing the entrapment of air.

Initial wetting cycles. The sensors were subjected to three wetting-drying cycles. During each wetting phase, the sensors were partially submerged (to less than 50% of their body length) for 30 minutes. Partial immersion allows air to escape through the dry pores while water is drawn into the internal matrix by capillary action. After each immersion, the sensors were removed and air-dried as indicated in the Figure 16.

A) Day 1 (Morning): 30-minute partial immersion, followed by air-drying until the evening.

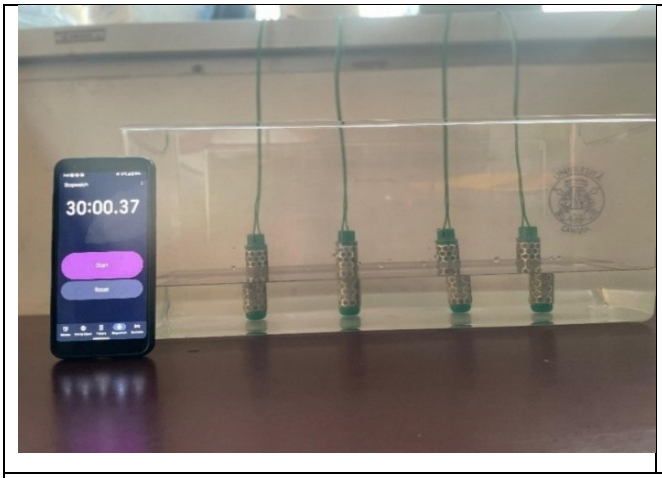

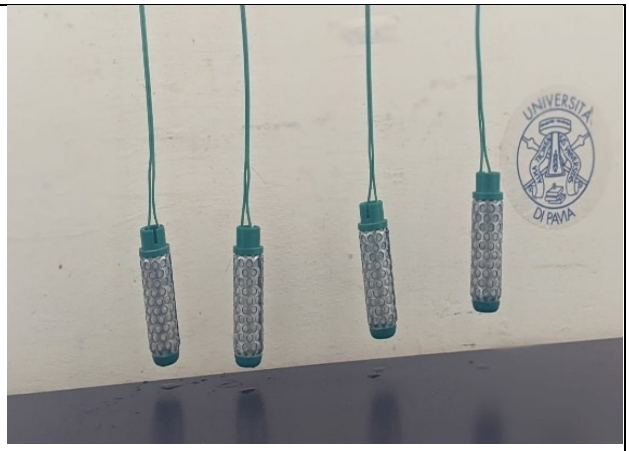

B) Day 1 (Evening): 30-minute partial immersion, followed by overnight air-drying.

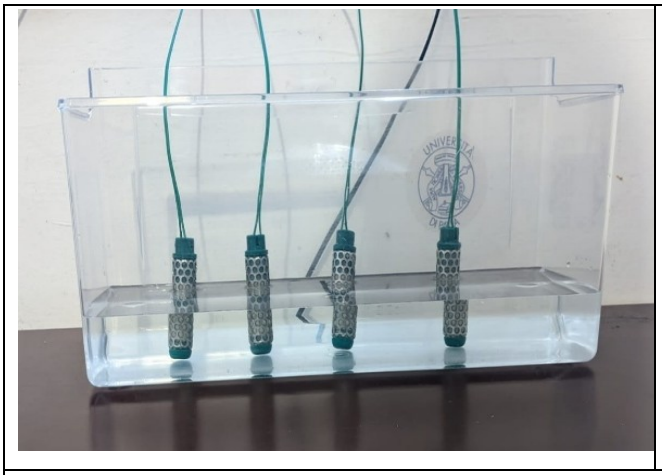

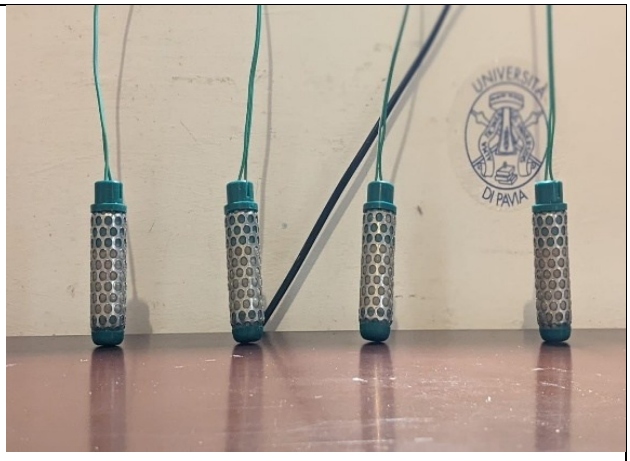

C) Day 2 (Morning): 30-minute partial immersion, followed by air-drying until the evening.

Figure 16: *Performance of the WATERMARK 200SS sensor during cyclic partial wetting and air-drying phases.*

Final Saturation and Installation. On the evening of the second day, the sensors were transitioned from partial immersion to full submersion for an overnight period to achieve complete saturation. On the third morning, the fully saturated sensors were integrated into the experimental assembly consisting of four testing stations. Each station used a container filled with 2,000 g of sand as the substrate. To establish specific moisture gradients for calibration, different water volumes were added to each container: 500 ml (100% saturation), 250 ml (50%), 100 ml (20%), and 50 ml (10%), as labelled on the test cylinders in the laboratory setup. The initial parameters are documented in Figure 17 (Section E).

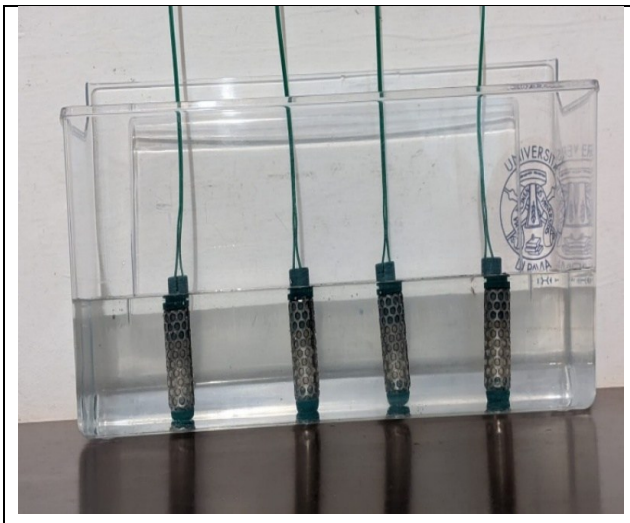	
D) On the evening of the second day, the sensors were fully submerged overnight.	**E)** After installation of the sensors and starting of data recording.

Figure 17: *The sensors were subjected to a final overnight submersion.*

The calibration phase was executed under controlled conditions to establish a baseline for sensor measurements across a spectrum of moisture gradients. To minimize potential variability associated with substrate porosity and density, a uniform sand substrate (2,000 g per container) was used. As summarized in Table 3, the experimental design incorporated four saturation levels (10%, 20%, 50%, and 100%), corresponding to volumetric water additions of 50 ml, 100 ml, 250 ml, and 500 ml, respectively. All sensors were deployed simultaneously on January 27, 2026, at 09:44 AM, with subsequent measurements recorded at 30-minute intervals.

Table 3: *Initial experimental conditions for sensor calibration in sand substrate.*

Sensor ID	Water Volume %	Water volume in the container (ml)	Soil type in the container	Soil in the container (g)	Sensor insertion time (h)	Sensor condition	Moisture profile
S1	100	500	Sand	2,000	09:44	Saturated	High Saturation
S2	50	250	Sand	2,000	09:44	Saturated	Moderate
S3	20	100	Sand	2,000	09:44	Saturated	Low
S4	10	50	Sand	2,000	09:44	Saturated	Minimum

2.9.2 Indoor calibration of WATERMARK 200ss soil moisture sensors

The Watermark 200SS sensors measure the electrical resistance (R) of a porous granular matrix that equilibrates with the surrounding soil moisture. The resistance value depends on the amount of water present within the sensor; as soil moisture decreases, the electrical resistance increases. To interpret these readings as soil water tension, a calibration equation can be used to convert resistance into matric potential (kPa or centibars).

In this study, the calibration procedure followed the empirical relationship developed by Clinton and Shock (1998), which relates resistance (R) in kilo-ohms (kΩ) and temperature (T) in degrees Celsius (°C) to soil water tension (kPa). The equation is expressed as:

$$\text{kPa}=\frac{-3.213*R-4.093}{1-0.009733*R-0.01205*T} \quad \text{(Eq.1)}$$

where: R is Sensor resistance (kΩ), T is Soil temperature (°C), and kPa is Soil water tension (1 kPa = 1 centibar).

This calibration covers the range of 10 to 100 kPa. Linear extrapolations are typically applied below 10 kPa and above 100 kPa. A fully saturated (wet) WATERMARK sensor typically measures approximately 550 ohms (0.55 kΩ), corresponding to soil tension near 0 kPa. Temperature affects resistance readings, as warmer conditions reduce resistance. To account for this effect, soil temperature was measured simultaneously using a digital temperature sensor. When temperature data are not available, a default value of 24°C can be used for approximate correction; however, for higher precision, the calibration equation should include measured temperature values. This approach allows conversion of measured resistance values into soil water tension values using the calibration equation (Website 15).

2.10 Overview and setup of the outdoor WATERMARK 200SS sensor validation activities

Following the indoor calibration phase, the sensors were installed in an experimental vineyard to evaluate their performance under field conditions. The field experiment was conducted in Pavia (Lombardy, northern Italy), where the climate is characterized by hot summers and relatively mild winters. Summer temperatures typically range between 25°C and 30°C, with occasional peaks above 35°C. Winter temperatures generally range between 5°C and 10°C. Rainfall is distributed throughout the year, with wetter periods usually occurring during spring and autumn months (Website 12). The experimental vineyard consisted of five Chardonnay grapevines cultivated in plastic pots. The vines

were spaced approximately 140 cm apart, allowing adequate spacing for plant growth and sensor installation. The grapevines were approximately two years old at the time of the experiment.

Each vine was grown in a rectangular plastic PPL container filled with a substrate composed of approximately 40% river sand and 60% soil. This substrate mixture was used to provide drainage conditions while maintaining structural stability for root development. The sandy component supported observation of moisture variations during sensor monitoring. For the outdoor validation experiment, soil moisture sensor was installed in one of the potted grapevines. The sensor was connected to the Arduino Edge Control monitoring system, which collected soil moisture measurements and transmitted them through the wireless communication module.

During the field experiment, the monitoring system was configured to record soil moisture measurements every 15 minutes, according to the data acquisition protocol defined during system configuration. This interval allowed continuous logging of soil moisture variations throughout the experiment.

A) River Sand and Soil used During the field experiment

B) Measuring of 40% river sand and 60% soil.

C) Mixing well of 40% river sand and 60% soil.

D) Sensor installation in 15 cm and calibration on field.

Figure 18: *Experimental vineyard illustrating the spacing and positioning of five Chardonnay grapevines in pots.*

2.11 Real-time meteorological monitoring via Davis Vantage pro 2 and Weatherlink systems

A) Davis Vantage Pro 2

B) Davis Instruments Weatherlink Touch Console 6313EU Wireless Digital Weather Station

Figure 19: *A) Integrated sensor suite (ISS) for atmospheric monitoring and (B) WeatherLink touch console (6313EU) for Real-time data visualization and cloud integration.*

The environmental monitoring system for this research even focused on the Davis Vantage Pro 2 Integrated Sensor Suite (ISS) and the WeatherLink Touch Console (6313EU), which together provide the high-frequency data necessary for precision irrigation management. The ISS, as illustrated in the first figure of Davis Vantage Pro 2, continuously monitors critical variables including Temperature °C, Rain (mm) and Average Wind Speed m/s, providing the foundational dataset required to calculate crop water needs (Website 18). As shown in the second figure of Davis Instruments Weatherlink Touch Console 6313EU Wireless Digital Weather Station, the WeatherLink Touch Console serves as the central hub for this network, revolutionizing data reporting through an intuitive interface and integrated Wi-Fi connectivity (Website 19). This console facilitates the seamless streaming of hyperlocal weather data to the WeatherLink cloud, a feature that is instrumental for the experimental calibration and validation of soil moisture sensors. By synchronizing atmospheric trends with subsurface Arduino-based monitoring data, this infrastructure supports a comprehensive "smart" approach to vineyard management, ensuring data accuracy for both immediate field operations and long-term analytical validation. And the reading was recording after each 5 minutes.

2.12 Comparison of soil moisture sensing for smart vineyard irrigation

The Xiaomi Smart Sensor Plant Flower Hydroponics Analyzer was used as a supplementary device to support data interpretation through comparative analysis. Unlike the WATERMARK 200SS sensors, which are scientifically validated and widely used in agricultural research, this low-cost sensor does not provide the same level of measurement accuracy or reliability. The device operates using a capacitive sensing probe that must be inserted into the soil to estimate moisture content, while the upper electronic housing remains dry. It provides simplified measurements of soil moisture (%), temperature (°C), and light intensity (lux), with data recorded at hourly intervals.

1

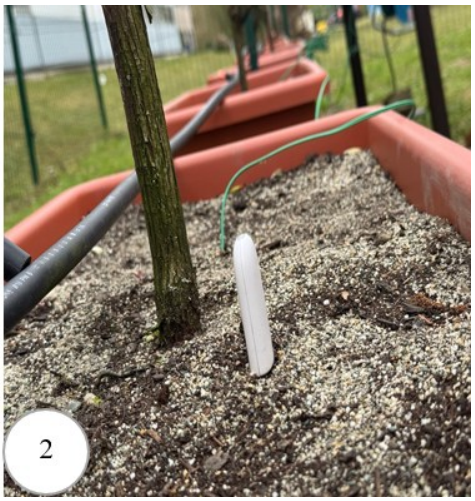

2

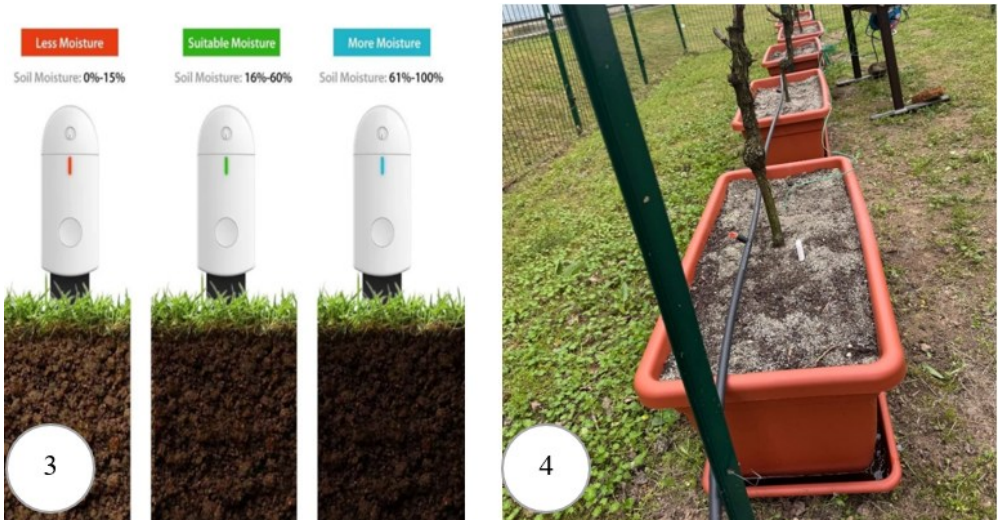

Figure 20: *Operational components and experimental application of the smart sensor soil moisture detector (1 and 3 from Website 20).*

Due to its limited precision and lack of scientific calibration, the sensor was not used as a primary measurement tool. Instead, it served as a qualitative reference to compare general moisture trends observed by the WATERMARK 200SS sensors. Although the device includes a basic tri-color LED system to indicate moisture conditions (dry, optimal, or saturated), these indicators were considered indicative rather than quantitative. Therefore, the role of this sensor in the study was limited to supporting the interpretation of soil moisture dynamics rather than providing validated measurements.

CHAPTER 3. RESULTS

3.1 Performance evaluation of WATERMARK 200ss sensors across variable moisture gradients

To evaluate sensor performance, WATERMARK 200SS soil moisture sensors (based on electrical resistance to infer soil water tension) were tested across four distinct moisture gradients within 2000 g sand substrates. The experiment was conducted from January 27 to February 3, 2026. The four moisture conditions were established using water volumes of 500 ml (25%), 250 ml (12.5%), 100 ml (5%), and 50 ml (2.5%), as shown in Figure 21. The results indicate a clear relationship between moisture level and sensor response. High-moisture conditions (Container 1 and Container 2) maintained low and stable resistance values, whereas drier substrates (Container 3 and Container 4) showed a progressive increase in resistance over time. In particular, Container 4 (2.5%) exhibited a sustained rise exceeding 600 Ω and was the only condition where soil tension readings were consistently activated, indicating the system's ability to distinguish between well-hydrated and severely depleted conditions.

Figure 21: *Humidity trend monitoring during the sensor performance evaluation phase.*

Table 4 summarizes the influence of initial water content on sensor behaviour. Sensors S1 and S2 maintained resistance values within a stable low range and did not reach irrigation trigger conditions. Sensor S3 showed a gradual increase toward higher resistance values, while S4 displayed the most pronounced increase, reaching a maximum of 622.5 Ω. Notably, S4 was the only sensor that triggered an irrigation event (February 2), confirming the effectiveness of the threshold-based detection system.

Table 4: *Summary of weekly sensor readings and irrigation trigger points across varying moisture levels.*

Sensor	Water (ml)	Avg. Resistance (R) (Ω)	Irrigation Trigger
S1	500	330 - 370	None
S2	250	330 - 370	None
S3	100	360 - 410	None
S4	50	360 - 620	Active (Feb 2nd)

The initial phase of the experiment (Table 5), corresponding to the first five hours of monitoring, established baseline conditions for all sensors. Resistance values remained within a narrow range (333.75–378.6 Ω), while all soil tension readings remained at 0 CB, indicating uniform initial moisture conditions across the substrates.

Table 5: *Baseline electrical resistance (R) and soil tension measurements (CB) for containers 1–4 during initial system calibration (January 27, 2026).*

Date & Time	R1	CB 1	R2	CB 2	R3	CB 3	R4	CB 4
2026-01-27 10:14:38	360.00	0	358.50	0	333.75	0	356.55	0
2026-01-27 10:14:39	363.20	0	362.20	0	359.85	0	362.25	0
2026-01-27 10:44:42	370.60	0	376.65	0	376.35	0	378.60	0
2026-01-27 10:44:43	378.40	0	376.10	0	376.30	0	375.80	0
2026-01-27 11:14:45	362.75	0	361.70	0	365.40	0	360.70	0
2026-01-27 11:14:46	363.85	0	363.50	0	361.35	0	363.45	0
2026-01-27 11:44:49	363.45	0	363.50	0	361.90	0	363.35	0
2026-01-27 11:44:50	363.20	0	364.20	0	362.05	0	363.45	0
2026-01-27 12:14:52	363.55	0	363.35	0	363.45	0	361.45	0
2026-01-27 12:14:53	363.85	0	363.70	0	362.05	0	364.95	0
2026-01-27 12:44:56	360.55	0	360.50	0	359.85	0	360.35	0
2026-01-27 12:44:57	362.70	0	363.80	0	362.30	0	362.25	0
2026-01-27 13:14:59	363.50	0	361.60	0	362.55	0	361.75	0
2026-01-27 13:15:00	363.05	0	362.85	0	360.35	0	361.80	0
2026-01-27 13:45:03	363.30	0	360.8	0	360.85	0	363.20	0
2026-01-27 13:45:04	362.65	0	369.15	0	362.25	0	362.10	0
2026-01-27 14:15:06	363.50	0	363.85	0	362.30	0	363.15	0
2026-01-27 14:15:07	363.50	0	362.45	0	360.90	0	361.95	0
2026-01-27 14:45:10	363.25	0	362.20	0	362.05	0	363.10	0
2026-01-27 14:45:11	365.15	0	362.25	0	360.00	0	364.15	0
2026-01-27 15:15:13	378.50	0	375.55	0	375.35	0	371.95	0

In contrast, the final phase (Table 6) captured the divergence between moisture conditions. While Sensors 1–3 maintained relatively stable resistance values and CB readings at zero, Sensor 4 consistently operated within a high-resistance range (600–622.5 Ω), with CB values activated at 1 CB. This confirms the separation between low-moisture stress conditions and higher moisture regimes.

Table 6: *High-Tension electrical resistance (R) and soil tension measurements (CB) during critical dehydration (February 3, 2026).*

Date & Time	R1	CB1	R2	CB2	R3	CB3	R4	CB4
2026-02-03 05:33:36	331.20	0	361.70	0	396.75	0	615.65	1
2026-02-03 06:03:39	331.35	0	361.80	0	393.30	0	613.55	1
2026-02-03 06:03:40	330.05	0	362.95	0	394.50	0	613.05	1
2026-02-03 06:33:42	331.65	0	362.50	0	391.75	0	618.55	1
2026-02-03 06:33:43	331.55	0	364.40	0	394.75	0	622.50	1
2026-02-03 07:03:46	333.55	0	374.65	0	407.65	0	615.60	1
2026-02-03 07:03:47	331.70	0	366.40	0	408.45	0	612.65	1
2026-02-03 07:33:49	346.80	0	345.40	0	408.55	0	607.45	1
2026-02-03 07:33:50	347.25	0	352.40	0	408.90	0	609.75	1
2026-02-03 08:03:53	347.50	0	343.95	0	407.15	0	603.95	1
2026-02-03 08:03:54	348.50	0	346.80	0	410.00	0	600.70	1
2026-02-03 08:33:56	337.60	0	354.95	0	414.90	0	600.55	1
2026-02-03 08:33:58	347.25	0	344.20	0	408.95	0	606.30	1
2026-02-03 09:04:00	332.20	0	363.15	0	401.65	0	616.30	1
2026-02-03 09:04:01	333.85	0	357.70	0	401.70	0	607.80	1
2026-02-03 09:34:04	329.45	0	362.25	0	396.95	0	612.05	1
2026-02-03 09:34:05	330.85	0	363.10	0	392.00	0	615.15	1
2026-02-03 10:04:07	331.75	0	363.40	0	393.35	0	615.30	1
2026-02-03 10:04:08	332.65	0	362.30	0	393.70	0	616.00	1
2026-02-03 10:34:11	330.55	0	361.20	0	397.65	0	611.70	1
2026-02-03 10:34:12	331.20	0	371.40	0	393.65	0	615.40	1

A) Experimental results for sensor performance in high-moisture conditions

Figure 22 illustrates the behaviour of Sensor 1 (25% moisture). Resistance remained stable within approximately 330–380 Ω, while CB values remained at 0 throughout the monitoring period. This confirms stable conditions in a highly hydrated substrate. A slight reduction in resistance observed toward the end of the experiment suggests progressive stabilization of the sensor–substrate interface. As moisture redistributed within the sand, electrical conductivity increased, resulting in a slight decrease in baseline resistance without affecting soil tension.

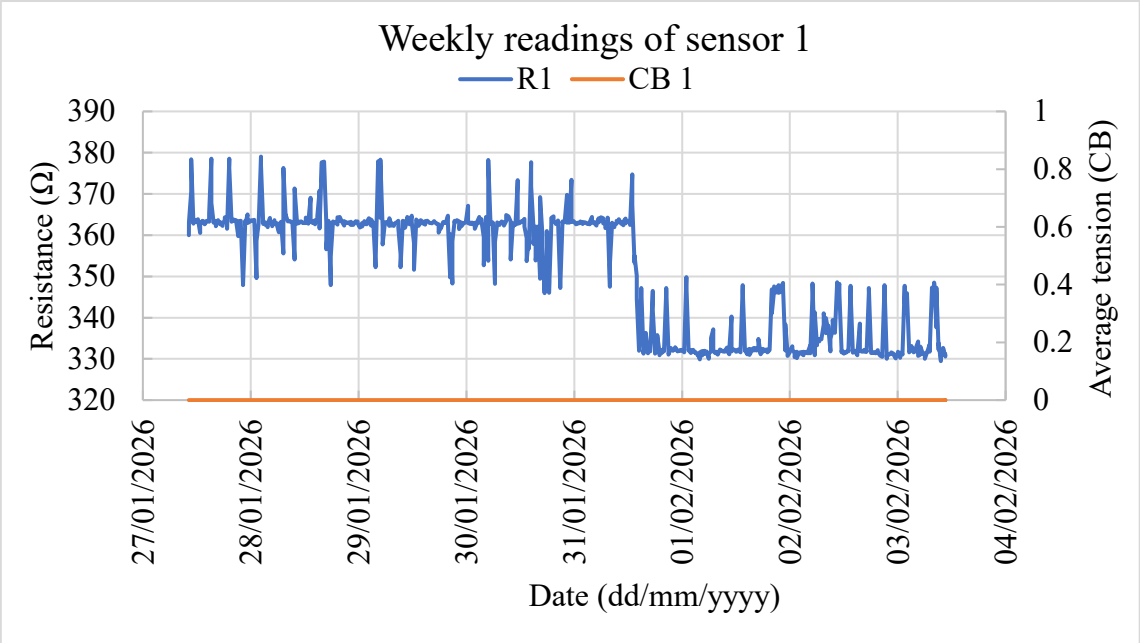

Figure 22: *Weekly resistance (Ω) and average soil tension (CB) readings for sensor 1 within container 1 with 25% moisture (500 ml) sand substrate, observed from January 27, 2026, to February 3, 2026.*

B) Experimental results for sensor performance in moderate moisture conditions

Sensor 2 (12.5% moisture), shown in Figure 23, exhibited behaviour consistent with Sensor 1. Resistance remained within a low baseline range (340–380 Ω), and CB values remained at 0. A temporary drop in resistance observed between February 1 and 2 reflects a localized wetting event. This response highlights the sensor's sensitivity to short-term moisture changes, followed by a return to baseline conditions as water redistributed within the substrate.

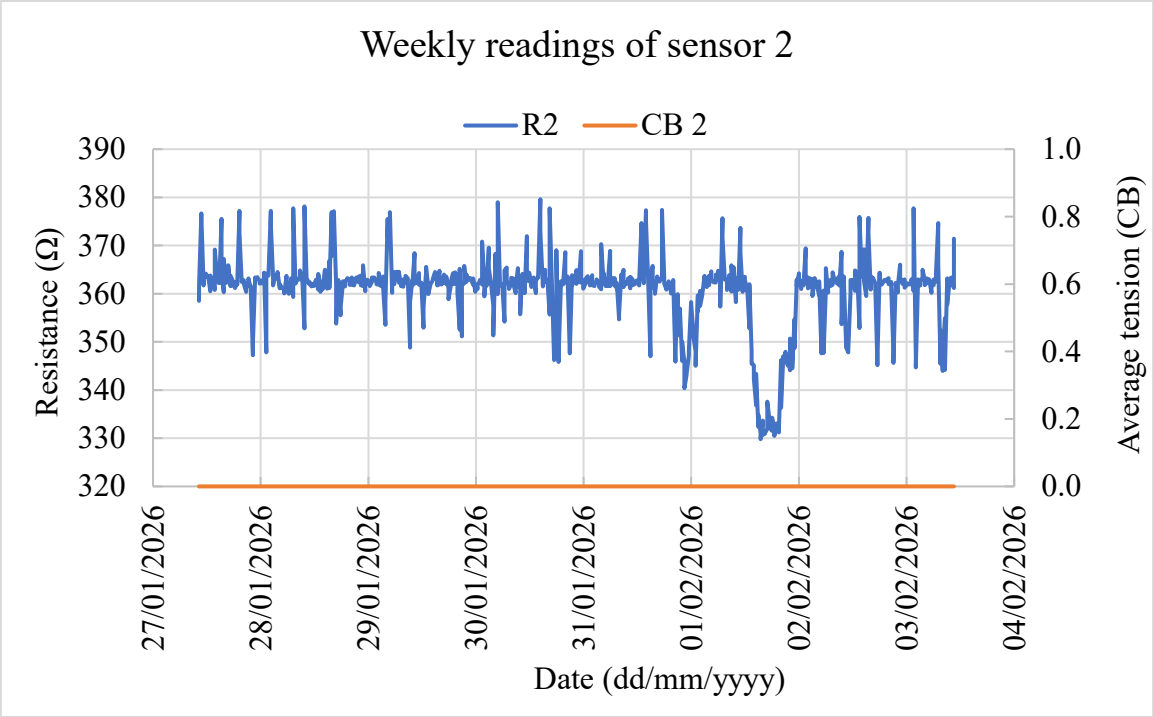

Figure 23: *Weekly resistance (Ω) and average soil tension (CB) readings for sensor 2 within container 2 with 12.5% moisture (250 ml) sand substrate, observed from January 27, 2026, to February 3, 2026.*

C) Experimental results for sensor performance under low moisture conditions

Figure 24 presents the behaviour of Sensor 3 (5% moisture). Resistance remained relatively stable (350–375 Ω) for most of the experiment, followed by a gradual increase toward 400 Ω in the final phase. This increase reflects progressive moisture depletion, reducing electrical conductivity. Despite this trend, CB values remained at 0, indicating that soil tension did not reach the activation threshold during the monitoring period.

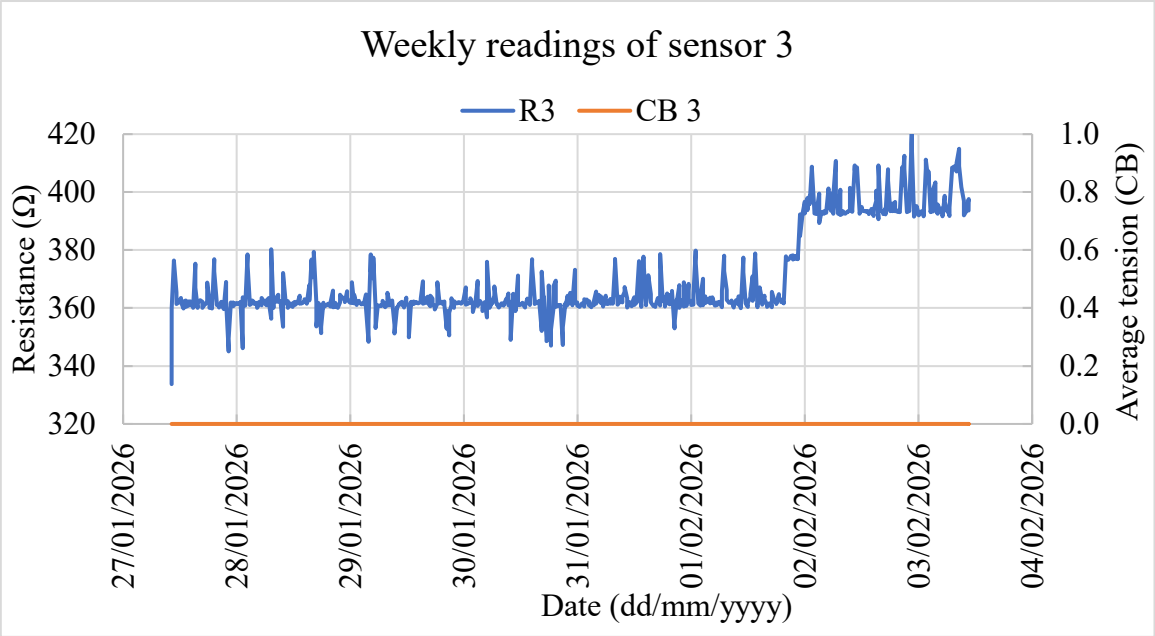

Figure 24: *Weekly resistance (Ω) and average soil tension (CB) readings for sensor 3 within container 3 with 5% moisture (100 ml) sand substrate, illustrating baseline stability and the onset of moisture depletion from January 27, 2026, to February 3, 2026.*

D) Experimental results for sensor performance under very low moisture conditions

Sensor 4 (2.5% moisture), shown in Figure 25, exhibited a distinct behaviour compared to the other conditions. Resistance increased continuously from appr approximately 360 Ω to values exceeding 600 Ω, reflecting progressive substrate drying. This condition was the only one where CB values were consistently activated (0.8–1.0), indicating the transition to a high-resistance regime associated with severe moisture depletion. This confirms the system's ability to detect stress conditions.

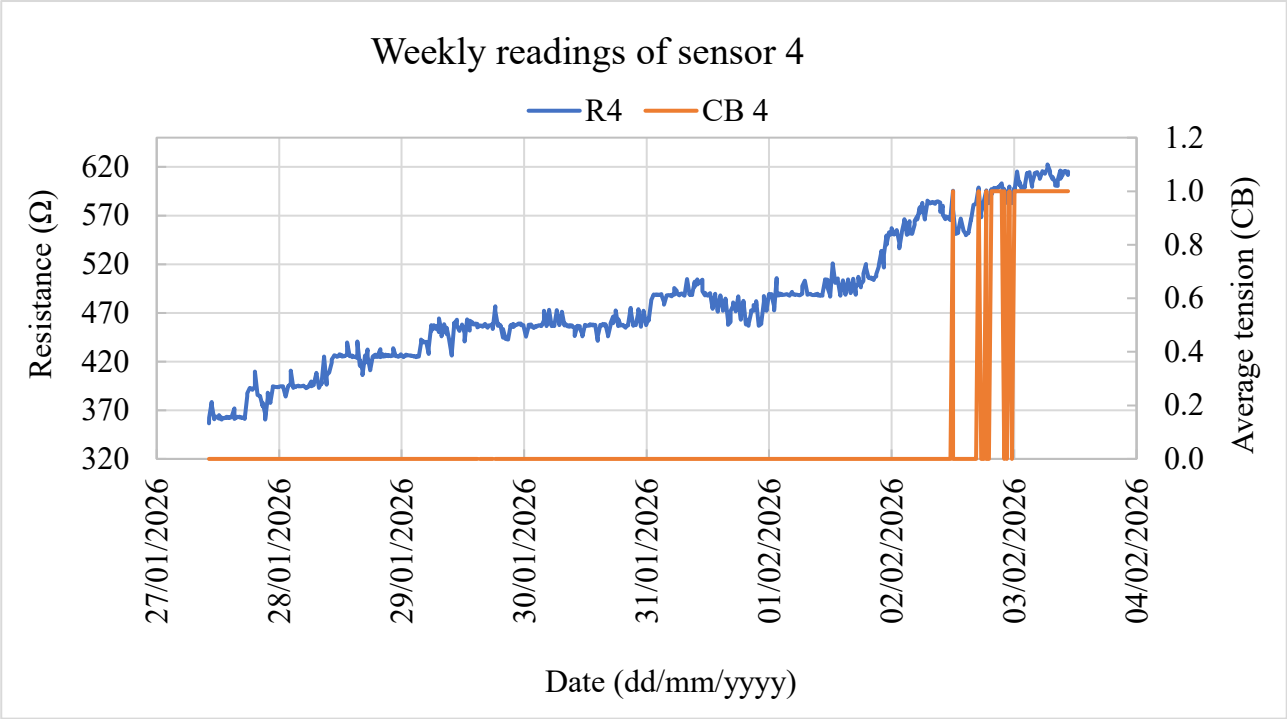

Figure 25: *Weekly resistance (Ω) and average soil tension (CB) readings for sensor 4 within container 4 with 2.5% moisture (50 ml) sand substrate, illustrating a linear resistance rise and the triggering of soil tension "stress points" from January 27, 2026, to February 3, 2026.*

E) Comparative analysis of sensor performance

The comparison across all moisture levels (Figure 26) confirms a consistent relationship between substrate moisture and resistance. High-moisture conditions (25% and 12.5%) maintained stable low resistance and CB values at 0, while lower moisture levels showed progressively higher resistance values. Only the lowest moisture condition (2.5%) triggered soil tension readings, clearly distinguishing it from the other treatments. Occasional resistance dips observed in wetter substrates correspond to temporary wetting events, followed by stabilization. Overall, the results demonstrate the ability of the system to differentiate moisture conditions across the tested gradients.

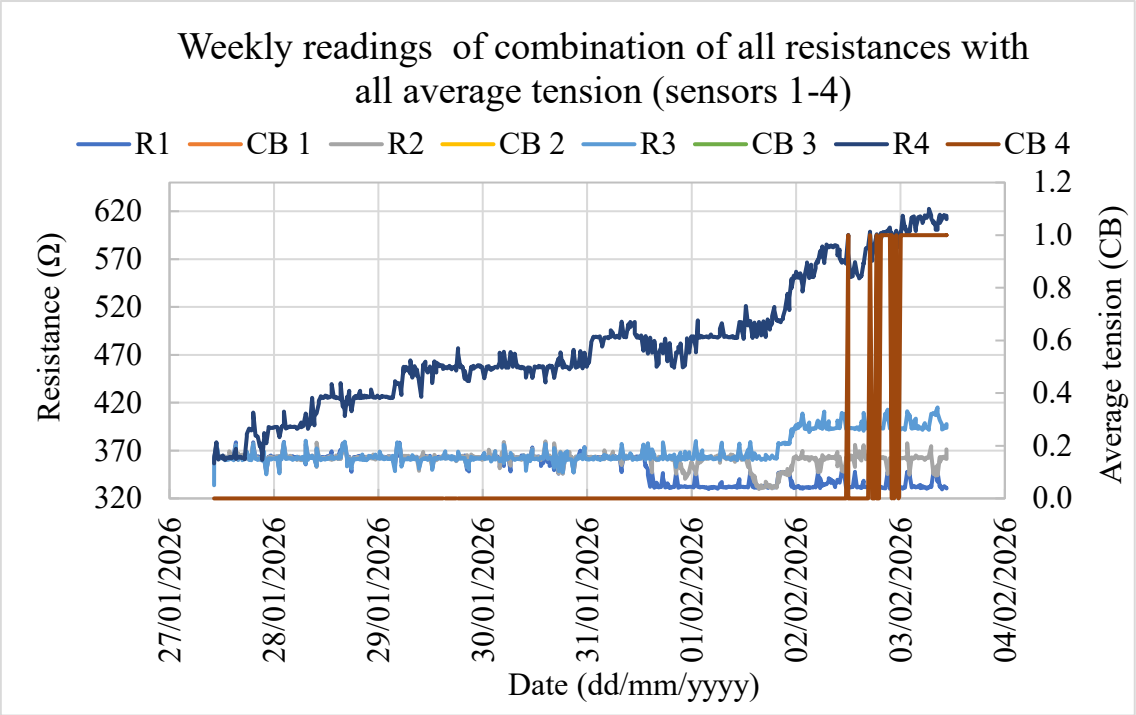

Figure 26: *Comprehensive weekly readings of electrical resistance (R1-R4) and average soil tension (CB 1-4) across 25%, 12.5%, 5%, and 2.5% moisture gradients in 2000 g sand substrates (Jan 27 – Feb 3, 2026).*

3.2 Correlation between soil resistance (R) and matrix tension (CB)

The graph illustrates the relationship between electrical resistance (Ω) and soil water tension (CB) during the outdoor monitoring period. Both parameters show closely aligned trends, confirming a strong correlation. At the beginning of the monitoring period (25–27 March 2026), resistance ranged between 15,000 and 18,000 Ω, corresponding to soil water tension values of approximately 100–120 CB, indicating dry soil conditions. On March 27, a rapid transition occurred. At 09:34, soil tension reached 92.4 CB. At 09:45, a controlled irrigation event (1 liter of water) was applied, resulting in an immediate drop in resistance and soil tension to near-zero levels. Following irrigation, both parameters remained stable at low values, indicating sustained high soil moisture conditions. Minor fluctuations did not indicate significant drying. These results confirm the strong relationship between resistance and soil tension and demonstrate the system's responsiveness to rapid changes in soil moisture.

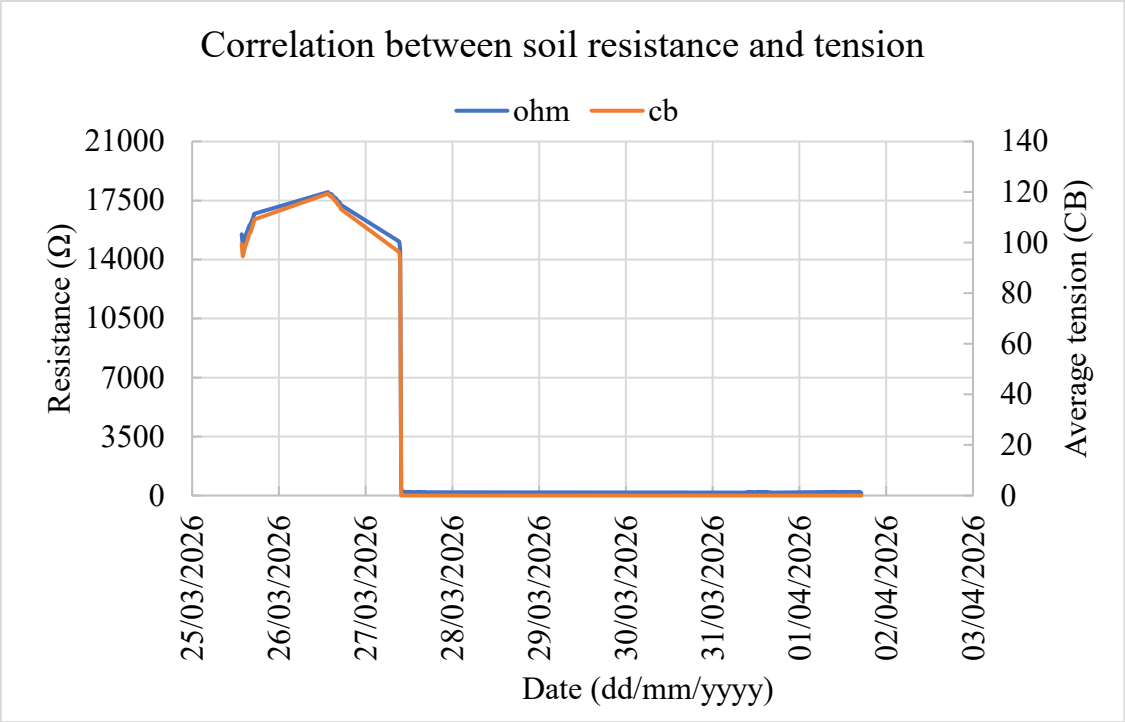

Figure 27: *Temporal correlation between electrical resistance (Ω) and tension (CB) in response to drying and saturation cycles.*

3.3 Comparative analysis of meteorological data and soil moisture response

The relationship between meteorological data and soil water tension was evaluated using data from the Davis Vantage Pro 2 weather station. On March 25, a rainfall event of approximately 0.22 mm was recorded. This produced only a minimal response in soil water tension, which remained between 95 and 120 CB, indicating limited impact on soil moisture. In contrast, the irrigation event on March 27 caused a sharp decrease in soil tension to approximately 0 CB, indicating saturation. After this event, soil moisture remained stable despite temperature fluctuations between 5°C and 22°C. These results highlight the difference between natural rainfall and irrigation, showing that only sufficient water input leads to significant changes in soil moisture conditions.

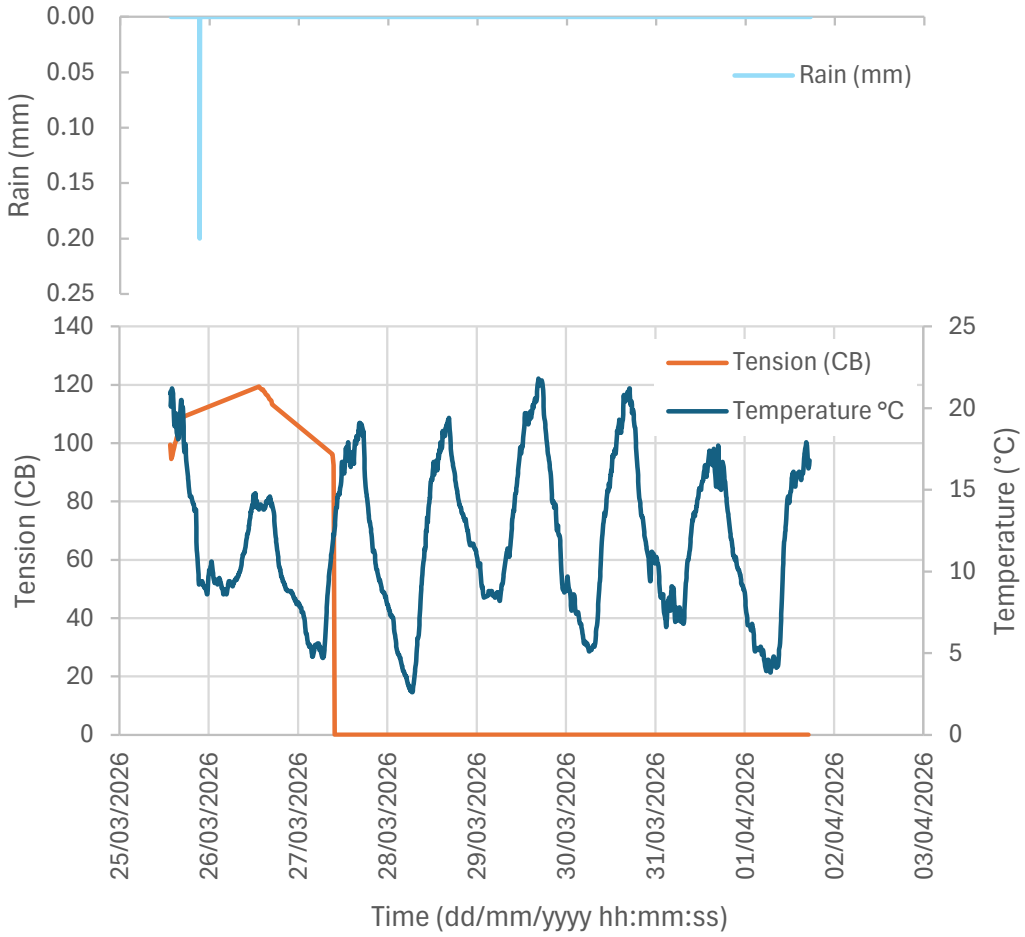

Figure 28: *Temporal variation of rainfall (mm), soil water tension (CB), and air temperature (°C) during the outdoor validation period. A minor rainfall event (0.22 mm) produced a negligible change in soil water tension, while a controlled irrigation event (1 L) resulted in a rapid decrease to approximately 0 CB, indicating soil saturation. Temperature shows regular diurnal fluctuations throughout the monitoring period.*

3.4 Performance correlation between WATERMARK 200SS matric potential and smart sensor volumetric moisture

The comparison between the WATERMARK 200SS sensor and the capacitive Xiaomi sensor highlights clear differences in performance. At the beginning of the monitoring period, the WATERMARK sensor recorded high soil tension values (100–120 CB), indicating dry conditions. In contrast, the Xiaomi sensor showed relatively stable values (18–21%) without clearly reflecting water stress. Following irrigation on March 27, the WATERMARK sensor showed an immediate drop to 0 CB, indicating saturation. The Xiaomi sensor, however, showed only moderate fluctuations without a clear response.

After irrigation, the WATERMARK sensor remained stable, while the Xiaomi sensor continued to fluctuate between 16% and 20%. These results indicate that the WATERMARK sensor provides a more consistent and sensitive response to soil moisture changes, while the Xiaomi sensor is more suitable for qualitative observations rather than precise measurements.

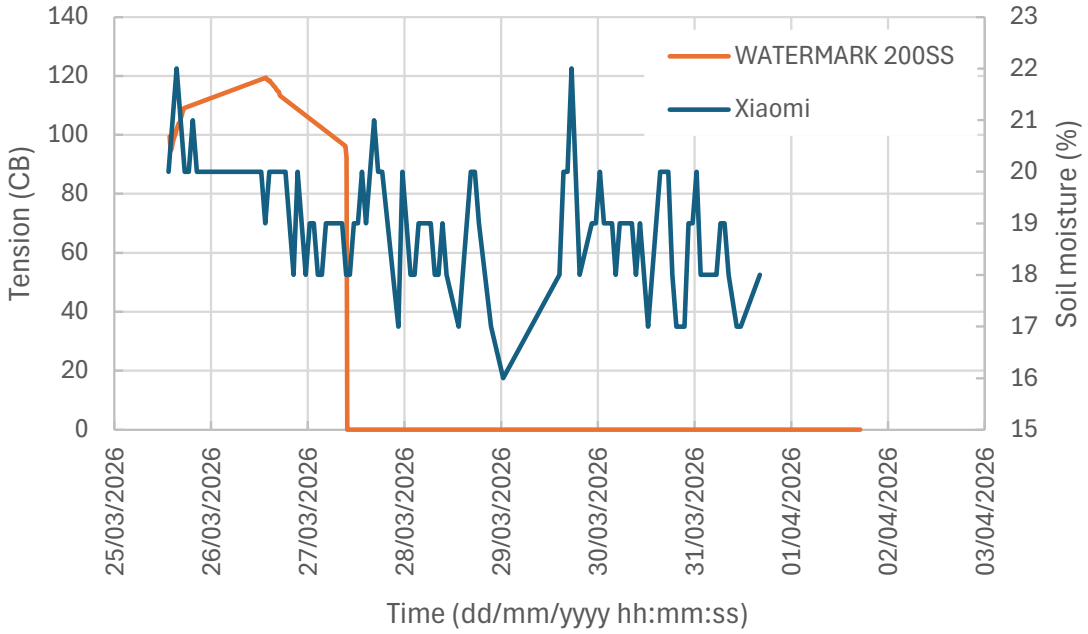

Figure 29: *Comparison between WATERMARK 200SS soil water tension (CB) and Xiaomi capacitive soil moisture (%) during the monitoring period, showing a sharper response of the WATERMARK sensor to irrigation and more variable trends in the low-cost sensor.*

CHAPTER 4. DISCUSSION

4.1 Performance evaluation of WATERMARK 200SS sensors across variable moisture gradients

The laboratory calibration phase provided a controlled framework to evaluate the behaviour of the WATERMARK 200SS sensors under predefined soil moisture conditions. The results clearly demonstrated a consistent and progressive relationship between soil water content and electrical resistance, which was subsequently translated into soil water tension values (CB). As the water content in the sand substrate decreased, the sensors exhibited a gradual increase in resistance, corresponding to higher matric tension values. This behaviour is fully coherent with the operating principle of granular matrix sensors, in which reduced water availability increases the electrical resistance within the porous medium (Shock et al., 1998). Across the different moisture treatments (25%, 12.5%, 5%, and 2.5%), the sensors were able to distinguish clearly between varying levels of soil water availability. In particular, higher moisture conditions resulted in relatively stable and low resistance values, while lower moisture contents produced a more pronounced increase in resistance, indicating progressive soil drying. The ability of the sensors to capture these gradients confirms their sensitivity across a wide range of soil moisture conditions, which is essential for irrigation management applications (Al-Sadi et al., 2024).

Moreover, the calibration results highlighted a relatively smooth and continuous transition between moisture levels, rather than abrupt or erratic changes. This indicates a stable sensor response and suggests that the WATERMARK 200SS sensors can provide reliable intermediate measurements, which are particularly important for identifying threshold conditions for irrigation scheduling (Shock et al., 1998).

It is also important to note that the use of a homogeneous sand substrate minimized external variability, allowing the intrinsic sensor behaviour to be evaluated without interference from soil heterogeneity. While this represents an idealized condition compared to field environments, it provides a necessary baseline for interpreting subsequent outdoor measurements (Li et al., 2009).

Overall, the laboratory calibration confirms that the WATERMARK 200SS sensors exhibit a predictable, stable, and sensitive response to soil moisture variations, supporting their use as reliable instruments for monitoring soil water status.

4.2 Correlation between soil resistance and matrix tension

The analysis of the relationship between electrical resistance (Ω) and soil water tension (CB) further reinforces the reliability of the WATERMARK 200SS sensors. The results showed a strong and consistent correlation between these two parameters, with both variables exhibiting nearly identical

temporal trends during the monitoring period. During the initial phase (25–27 March 2026), high resistance values (approximately 15,000–18,000 Ω) corresponded to elevated soil water tension values (100–120 CB), indicating dry soil conditions and significant water stress. This agreement confirms that electrical resistance can be effectively used as a proxy for soil water tension, provided that appropriate calibration relationships are applied (Shock et al., 1998). A key observation in this dataset is the abrupt transition recorded on March 27. Just before this event, at 09:34, the sensor measured a soil water tension of 92.4 CB, reflecting a condition of moderate to severe water stress. Shortly after, at 09:45, a controlled irrigation event was applied, consisting of 1 liter of water. This intervention resulted in an immediate and drastic reduction in both resistance and soil water tension, with values dropping to near-zero levels. This sharp transition highlights two important aspects. First, it demonstrates the high responsiveness of the sensor system to rapid changes in soil moisture conditions. Second, it confirms that the sensors are capable of accurately capturing irrigation events, distinguishing them clearly from gradual drying processes (Al-Sadi et al., 2024). Following the irrigation event, both resistance and soil tension remained close to zero for the remainder of the monitoring period, indicating sustained high soil moisture conditions. This plateau suggests that the applied water volume was sufficient to maintain near-saturation conditions over time, at least within the monitored soil volume. Minor fluctuations observed after the irrigation event may be attributed to environmental factors such as temperature variations, evaporation, or slight redistribution of water within the substrate (Keller, 2020). However, these variations did not significantly alter the overall moisture status. In summary, the strong correlation between resistance and soil water tension, combined with the system's ability to detect rapid transitions, confirms the robustness of the WATERMARK 200SS sensors and validates the calibration approach adopted in this study.

4.3 Comparative analysis of meteorological data and soil moisture response

The integration of meteorological data with soil moisture measurements provides important insights into the relationship between atmospheric conditions and soil water dynamics. The results indicate that soil water tension responds differently to natural rainfall events compared to controlled irrigation, highlighting the importance of combining environmental and soil-based measurements in irrigation management (Mirás-Avalos & Araujo, 2021). A rainfall event of 0.22 mm was recorded on March 25. Despite being clearly detected by the weather station, this precipitation had only a minimal effect on soil water tension, which remained within a relatively high range (approximately 95–120 CB). This observation indicates that such a small rainfall amount was insufficient to significantly infiltrate the soil and alter the moisture conditions at the sensor depth. In contrast, the controlled irrigation event on March 27 resulted in a drastic reduction in soil water tension to approximately 0 CB. This

demonstrates that irrigation can produce a much stronger and more immediate impact on soil moisture compared to low-intensity rainfall events (Al-Sadi et al., 2024). The difference between these two responses highlights the importance of considering not only precipitation occurrence but also its magnitude and effectiveness in influencing soil water availability.

Temperature data further support the interpretation of soil moisture dynamics. The recorded temperature exhibited clear daily fluctuations, reflecting diurnal cycles. These variations can influence soil moisture through evaporation and plant transpiration processes (Keller, 2020). However, despite these temperature fluctuations, soil water tension remained stable at low values after the irrigation event, indicating that the soil retained sufficient moisture to buffer short-term atmospheric demand. This finding suggests that once field capacity conditions are reached, short-term variations in temperature may not immediately translate into significant changes in soil water tension, particularly in the absence of strong evaporative demand or plant uptake. Overall, the combined analysis of meteorological and soil data demonstrates that the monitoring system is capable of distinguishing between different hydrological processes and provides a comprehensive understanding of soil water dynamics in response to both environmental and controlled inputs.

4.4 Performance correlation between WATERMARK 200SS and low-cost capacitive sensor

The comparison between the WATERMARK 200SS sensors and the capacitive low-cost sensor (Smart Sensor Plant Flower Hydroponics Analyzer) provides valuable insights into the reliability and limitations of different soil moisture sensing technologies. The WATERMARK sensors, based on the measurement of soil water tension, showed a clear and physically meaningful response to changes in soil moisture conditions. In particular, the transition from dry conditions to saturation was sharply defined, with soil tension dropping rapidly to 0 CB following the irrigation event. This behaviour reflects the direct relationship between matric potential and plant-available water (Keller, 2020). In contrast, the capacitive sensor, which measures volumetric soil moisture content, exhibited a more variable and less stable signal. Although general trends in soil moisture variation could be observed, the sensor did not show a clear or immediate response to the irrigation event comparable to that of the WATERMARK sensors. Instead, its readings fluctuated within a relatively narrow range, making it more difficult to identify precise changes in soil water status. This difference can be attributed to several factors. Capacitive sensors are typically more sensitive to soil properties such as texture, salinity, and temperature, and they often require site-specific calibration to provide accurate measurements. In addition, low-cost devices are generally designed for qualitative rather than quantitative monitoring, which limits their applicability in precision irrigation systems (Al-Sadi et al., 2024).

Despite these limitations, the capacitive sensor still provided useful complementary information, particularly for identifying general moisture trends. Its simplicity, low cost, and ease of use make it a potentially valuable tool for preliminary monitoring or for applications where high precision is not required. However, for irrigation management purposes, where accurate detection of soil water thresholds is critical, the WATERMARK 200SS sensors demonstrated significantly higher reliability and performance.

4.5 Synthesis: implications for smart irrigation in viticulture

The combined results of this study highlight the potential of integrating calibrated soil moisture sensors within an Arduino-based monitoring system for precision irrigation in vineyards. The WATERMARK 200SS sensors proved to be reliable across both laboratory and field conditions, demonstrating strong sensitivity to soil moisture variations, rapid responsiveness to irrigation events, and stable long-term performance (Shock et al., 1998; Al-Sadi et al., 2024). The integration with the Arduino Edge Control platform enabled continuous data acquisition with a suitable temporal resolution (15-minute interval), ensuring that both gradual and rapid changes in soil water conditions were effectively captured. One of the most relevant outcomes of this study is the system's ability to distinguish between ineffective rainfall events and effective irrigation inputs. This capability is essential for optimizing irrigation scheduling, as it prevents unnecessary water application and supports more efficient water use. Furthermore, the results emphasize the importance of sensor selection in smart irrigation systems. While low-cost sensors may provide general trends, their limitations in accuracy and stability make them less suitable for decision-making processes that require precise thresholds. From a broader perspective, the implementation of such monitoring systems represents a key step toward data-driven irrigation management, which is increasingly necessary under climate change conditions characterized by higher temperatures and more frequent droughts (Naumann et al., 2021; Challinor et al., 2014).

CHAPTER 5. CONCLUSION

This study evaluated the performance of WATERMARK 200SS soil moisture sensors integrated with an Arduino Edge Control system for vineyard irrigation monitoring. The research focused on the experimental calibration and validation of the sensors through a combined laboratory and field approach, with the aim of assessing their reliability, responsiveness, and applicability in precision agriculture.

The laboratory calibration demonstrated that the sensors provide a consistent and stable response across a range of soil moisture conditions. A clear relationship between electrical resistance and soil water tension was observed, confirming the suitability of the sensors for detecting variations in soil water availability. The controlled experimental setup allowed for the identification of well-defined response patterns, which served as a reference for interpreting field measurements. The outdoor validation phase confirmed the effectiveness of the sensors under real environmental conditions. The monitoring system successfully captured both gradual soil drying processes and rapid changes in moisture associated with irrigation events. In particular, the sharp decrease in soil water tension following the application of 1 liter of water demonstrated the high sensitivity and responsiveness of the sensors, highlighting their capability to detect real-time changes in soil conditions. The integration of meteorological data further improved the understanding of soil moisture dynamics. The results showed that low-intensity rainfall had a negligible effect on soil water tension, while controlled irrigation produced a rapid and significant response. This distinction is particularly relevant for irrigation management, as it allows for a more accurate evaluation of effective water inputs. The comparison with a low-cost capacitive sensor highlighted the importance of sensor selection in precision agriculture systems. While the low-cost sensor was able to capture general trends, it showed greater variability and lower sensitivity compared to the WATERMARK 200SS sensors. This confirms that low-cost devices are more suitable for qualitative observations, whereas calibrated sensors are required for accurate irrigation monitoring.

Overall, the findings of this study demonstrate that WATERMARK 200SS sensors, when properly calibrated and integrated into an Arduino-based monitoring system, represent a reliable and effective tool for soil moisture monitoring in vineyards. This approach supports data-driven irrigation management, contributing to improved water-use efficiency and providing a practical solution to address the challenges posed by climate change in viticulture.

REFERENCES

Website 1 https://climate.ec.europa.eu/climate-change/causes-climate-change_en

Website 2 https://climate.ec.europa.eu/climate-change/consequences-climate-change_en

Website 3 https://grapes.extension.org/what-is-a-vineyard/

Website 4 https://wineinternationalassociation.org/top-30-wineries-in-italy/

Website 5 https://vineyards.com/wine-map/italy

Website 6 https://www.guadoalmelo.it/en/cambio-climatico-e-viticoltura-scelte-opportune-o-irresponsabili/

Website 7 https://esi.com.my/inst-home/irrometer-tensiometer/

Website 8 https://www.irrometer.com/basics.html

Website 9 https://www.elprocus.com/smart-irrigation-system-using-iot/

Website 10 https://winechannel.it/the-use-of-internet-of-things-iot-in-the-world-of-wine/

Website 11 https://ieeexplore.ieee.org/abstract/document/8473292

Website 12 https://www.nearweather.com/location/3171366

Website 13 https://store.arduino.cc/products/arduino-edge-control

Website 14 https://www.yuasa.co.uk/np7-12.html

Website 15 https://www.irrometer.com/200ss.html

Website 16 https://docs.arduino.cc/tutorials/edge-control/watermark-adapter-setup/

Website 17 https://docs.arduino.cc/software/ide-v2/tutorials/getting-started-ide-v2/

Website 18: https://www.meteoproject.it/davis-vantage-pro2.php

Website 19: https://www.conrad.it/it/p/davis-instruments-weatherlink-touch-console-6313eu-stazione-meteo-digitale-senza-fili-numero-di-sensori-max-80-3123439.html

Website 20 https://daddysdeals.co.za/deals/not-rated/vouchers/smart-sensor-plant-flower-hydroponics-analyzer-and-detector/

Adams, R. M., Hurd, B. H., Lenhart, S., & Leary, N. (1998). Effects of global climate change on agriculture: An interpretative review. *Climate Research, 11*(1), 19–30. https://doi.org/10.3354/cr011019

Al-Sadi, A. M., Al-Azri, M., & Al-Mahmooli, I. H. (2024). Smart irrigation systems for sustainable agriculture: A review of recent developments. *Agronomy, 14*(7), 1360. https://doi.org/10.3390/agronomy14071360

Bosello, F., & Zhang, J. (2005). *Assessing climate change impacts: Agriculture* (FEEM Working Paper No. 94.05). Fondazione Eni Enrico Mattei.

Cao, L., Bala, G., Caldeira, K., Nemani, R., & Ban-Weiss, G. (2010). Importance of carbon dioxide physiological forcing to future climate change. *Proceedings of the National Academy of Sciences, 107*(21), 9513–9518. https://doi.org/10.1073/pnas.0913000107

Challinor, A. J., Watson, J., Lobell, D. B., Howden, S. M., Smith, D. R., & Chhetri, N. (2014). A meta-analysis of crop yield under climate change and adaptation. *Nature Climate Change, 4*(4), 287–291. https://doi.org/10.1038/nclimate2153

Deutsch, C. A., Tewksbury, J. J., Tigchelaar, M., Battisti, D. S., Merrill, S. C., Huey, R. B., & Naylor, R. L. (2018). Increase in crop losses to insect pests in a warming climate. *Science, 361*(6405), 916–919. https://doi.org/10.1126/science.aat3466

Eekhout, J. P., & de Vente, J. (2022). Global impact of climate change on soil erosion and potential for adaptation through soil conservation. Earth-Science Reviews, 226, 103921. https://doi.org/10.1016/j.earscirev.2022.103921

Gambarani, A., Bordoni, M., Giganti, M., Vivaldi, V., Gatti, M., Poni, S., Vercesi, A., & Meisina, C. (2026). Multi-Year Assessment of Soil Moisture Dynamics Under Nature-Based Vineyard Floor Management in the Oltrepò Pavese (Northern Italy). Agriculture, 16(3), 316. https://doi.org/10.3390/agriculture16030316

Gay, C., Estrada, F., Conde, C., Eakin, H., & Villers, L. (2006). Potential impacts of climate change on agriculture: A case of coffee in Veracruz, Mexico. *Climatic Change, 79*(3-4), 259–288. https://doi.org/10.1007/s10584-006-9066-x

Gray, S. B., & Brady, S. M. (2016). Plant developmental responses to climate change. *Developmental Biology, 419*(1), 64–77. https://doi.org/10.1016/j.ydbio.2016.07.005

Kang, Y., Khan, S., & Ma, X. (2009). Climate change impacts on crop yield, crop water productivity and food security – A review. *Progress in Natural Science, 19*(12), 1665–1674. https://doi.org/10.1016/j.pnsc.2009.03.001

Karimi, V., Karami, E., & Keshavarz, M. (2018). Climate change and agriculture: Impacts and adaptive responses in Iran. *Journal of Integrative Agriculture, 17*(1), 1–15. https://doi.org/10.1016/S2095-3119(17)61794-5

Karki, S., Burton, P., & Mackey, B. (2020). The experiences and perceptions of farmers about the impacts of climate change and variability on crop production: A review. Climate and Development, 12(1), 80–95. https://doi.org/10.1080/17565529.2019.1603096

Keller, M. (2020). *The science of grapevines* (3rd ed.). Academic Press.

Kumar, R., & Gautam, H. R. (2014). Climate change and its impact on agricultural productivity in India. *Journal of Climatology & Weather Forecasting, 2*(1), 1–3. https://doi.org/10.4172/2332-2594.1000109

Li, Y. P., Huang, G. H., & Nie, S. L. (2009). An interval-parameter multi-stage stochastic programming model for water resources management under uncertainty. *Advances in Water Resources, 32*(10), 1439–1453. https://doi.org/10.1016/j.advwatres.2009.06.008

Mahato, A. (2014). Climate change and its impact on agriculture. *International Journal of Scientific and Research Publications, 4*(4), 1–6.

Mendelsohn, R. (2009). The impact of climate change on agriculture in developing countries. Journal of Natural Resources Policy Research, 1(1), 5–19. https://doi.org/10.1080/19390450802495882

Mirás-Avalos, J. M., & Araujo, P. M. (2021). Optimization of vineyard water management: Challenges, strategies, and technologies. *Agronomy, 11*(5), Article 826. https://doi.org/10.3390/agronomy11050826

Molua, E. L., & Lambi, C. M. (2007). *The economic impact of climate change on agriculture in Cameroon* (Policy Research Working Paper No. 4364). The World Bank.

Monteleone, B., Borzí, I., Bonaccorso, B., & Martina, M. (2023). Quantifying crop vulnerability to weather-related extreme events and climate change through vulnerability curves. Natural Hazards, 116(3), 2761–2796. https://doi.org/10.1007/s11069-022-05791-0

Naumann, G., Cammalleri, C., Mentaschi, L., & Feyen, L. (2021). Increased economic drought impacts in Europe with anthropogenic warming. *Nature Climate Change, 11*(6), 485–491. https://doi.org/10.1038/s41558-021-01037-x

NOAA National Centers for Environmental Information. (2023). Monthly global climate report for annual 2023. https://www.ncei.noaa.gov/access/monitoring/monthly-report/global/202313

Quénol, H., Garcia de Cortazar-Atauri, I., Duchêne, E., Richard, Y., Vigneau, J. P., & Bois, B. (2020). Viticultural adaptation to climate change. ISTE Ltd & Wiley.

Rosenzweig, C., & Liverman, D. (1992). Predicted effects of climate change on agriculture: A comparison of temperate and tropical regions. In S. K. Majumdar, L. S. Kalkstein, B. Yarnal, E. W. Miller, & L. M. Rosenfeld (Eds.), *Global Climate Change: Implications, Challenges and Mitigation Measures* (pp. 342–361). Pennsylvania Academy of Science.

Shock, C. C., Barnum, J. M., & Seddigh, M. (1998). Calibration of Watermark soil moisture sensors. Proceedings of the International Irrigation Show.

Stevanović, M., Popp, A., Lotze-Campen, H., Dietrich, J. P., Bodirsky, B. L., Bonsch, M., Popp, K., Humpenöder, F., & Weindl, I. (2016). The impact of high-end climate change on agricultural welfare. *Science Advances, 2*(8), Article e1501452. https://doi.org/10.1126/sciadv.1501452

Van Leeuwen, C., & Darriet, P. (2016). The Impact of Climate Change on Viticulture and Wine Quality. Journal of Wine Economics, 11(1), 150–167. https://doi.org/10.1017/jwe.2015.21

Waha, K., Müller, C., Bondeau, A., Dietrich, J. P., Kurukulasuriya, P., Heinke, J., & Lotze-Campen, H. (2013). Adaptation to climate change through the choice of cropping system and sowing date in sub-Saharan Africa. *Global Environmental Change, 23*(1), 130–143. https://doi.org/10.1016/j.gloenvcha.2012.11.001